

MASTER

ReBCO-based superconducting switch for high current applications

Garfias Davalos, D.A.

Award date:
2018

[Link to publication](#)

Disclaimer

This document contains a student thesis (bachelor's or master's), as authored by a student at Eindhoven University of Technology. Student theses are made available in the TU/e repository upon obtaining the required degree. The grade received is not published on the document as presented in the repository. The required complexity or quality of research of student theses may vary by program, and the required minimum study period may vary in duration.

General rights

Copyright and moral rights for the publications made accessible in the public portal are retained by the authors and/or other copyright owners and it is a condition of accessing publications that users recognise and abide by the legal requirements associated with these rights.

- Users may download and print one copy of any publication from the public portal for the purpose of private study or research.
- You may not further distribute the material or use it for any profit-making activity or commercial gain

ReBCO-based superconducting switch for high current applications

MSc Science and Technology of Nuclear Fusion

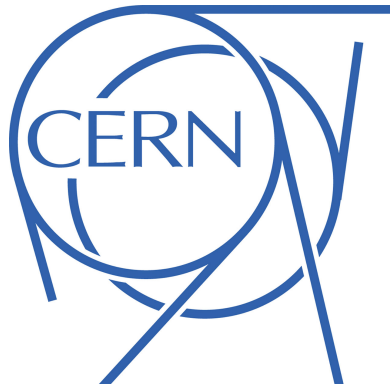
Diego Armando Garfias Dávalos

Supervisors:

H.H.J ten Kate (UT, CERN) and A. Dudarev (CERN)

N.J. Lopes Cardozo (TU/e)

Project developed at the
Experimental Physics Department
ATLAS Detector Operation Group
(EP - ADO)



Contents

List of Figures	iii
List of Tables	vi
Glossary	vii
Acronyms	viii
Abstract	viii
1 Introduction	1
1.1 Brief energy panorama	1
1.2 Superconductivity	2
1.3 Relevance of Superconductivity in Nuclear Fusion	4
1.4 Project Definition and Research Question	5
2 Superconductivity Technology Progress	8
2.1 Superconductivity concepts	8
2.1.1 Type I and Type II Superconductors	8
2.1.2 Resistivity and Critical Temperature	9
2.1.3 Operating in superconducting conditions	10
2.1.4 Power Law Equation	11
2.2 HTS Tapes	12
2.3 High current ReBCO Cables	13
2.3.1 ReBCO based Cable Concepts	13
2.3.2 CORC-type High Current ReBCO Cable	14
2.4 Status of HTS Technology for Nuclear Fusion Applications	15
2.5 Superconducting Switch Applications	17
2.5.1 Quench protection circuits	17
2.5.2 Superconducting Rectifier	18
3 Basis to build a ReBCO based superconducting switch	20
3.1 Superconducting switch principle	20
3.2 Superconducting switch with ReBCO tapes	21
3.2.1 Single switch	22
3.2.2 Double switch	23
3.3 Experimental test stand for ReBCO switch	23
3.4 Coating of ReBCO tapes	25
3.4.1 Stabilizer layers in ReBCO switch application	26
3.4.2 Etching	26
4 Simulation model of the ReBCO switch	28
4.1 One tape stack model	28
4.1.1 Thermal model 1D	28
4.1.2 Electrical model	28

4.2	Two conducting lines model	31
4.3	Considerations for a high electric current ReBCO switch	33
4.3.1	Vertical tape stacking	33
4.3.2	Interlayer thermal contact	34
4.3.3	2D Magnetic field	35
5	Results	37
5.1	Model tuning process	37
5.2	Simulation Output	38
5.2.1	Thermal response	38
5.2.2	Resistance over length	40
5.2.3	Time response	41
5.2.4	Current sharing between two conducting lines and power losses	42
5.2.5	Magnetic field	44
5.3	Measurements in test stand	47
5.3.1	Resistance per unit length	47
5.3.2	Time response	48
6	High current ReBCO switch proposal	50
6.1	Superconducting rectifier as goal for design	50
6.2	10 kA rated ReBCO-based superconducting switch	50
7	Summary and Discussion	53
7.1	Summary	53
7.2	Discussion	54
8	Conclusion	58
	Acknowledgements	59
	References	60

List of Figures

1	Diagram B vs T for Type I and Type II superconductors, critical values B_c and T_c are codependent limits to the transition to the normal conducting state. There's a sharp state change in Type I superconductors, and a transition region for Type II. From [26].	9
2	Schematic for Resistivity vs Temperature, showing the transition from superconducting to normal conducting states when exceeding the critical temperature of a Type II superconductor. Left: Mixed state between $T_{c,0}$ and $T_{c,onset}$, while getting to a temperature lower than $T_{c,0}$ makes virtually all resistance in the material to disappear [4]. Right: Resistivity vs Temperature for a LaSrCuO material, showing zoom-in in the transition temperature window of about 2 K between superconducting and normal conducting states [27].	9
3	Schematic for the critical surface in a Type II superconducting material, where T, B and j are interdependent values. To operate in superconducting state it is necessary to stay below the critical surface. Any point of the critical value correspond then to three interdependent values of T_c, B_{c2} and j_c . Adapted from [5].	10
4	Schematic of Current density vs Temperature, for the operating point of a superconductor at a fixed magnetic field value B_{op} . Δj and ΔT are the safety margins from the critical surface, shown here as a 2D cut with the line that joins T_c and j_c , which is part of the critical surface. From [4].	11
5	Schematic for Electric field vs Current density, to show the definition of the critical current density j_c in a superconductor, as the value where the electric field criterion E_0 is reached. Adapted from [30].	12
6	Schematic for a ReBCO tape. Note that the superconductor material is only a small fraction of the total thickness, and also includes regular conductor stabilizer layers. Design by SuperPower Inc. From [31].	13
7	Different types of proposed ReBCO cables by different research groups. (a) Twisted stacked-tape conductor (TSTC). (b) Roebel cable. (c) Round twisted stacked conductor. (d) ReBCO cable-in-conduit conductor. (e) Stacked tapes assembled in rigid structure conductor. (f) HTS-CrossConductor (HTS-CroCo). Adapted from [38].	14
8	CORC cable production: a) ReBCO tape wounded in round conductor, b) Winding of multiple ReBCO tapes in round conductor, c) Different diameter CORC cables, d) CORC-CICC for high current applications. Adapted from [20].	15
9	ARC reactor, featuring modular <i>HTS</i> coils, a liquid blanket, and vertical assembly for facilitating access and maintenance, with a major radius of 3.3 [m]. From [42].	16
10	Schematic for a basic persistent mode, quench protection circuit with superconductor switch. The switch in normal operation is cold (hence superconducting), so the current flows unimpeded through it. When the switch is heated up its resistance increases, and the electric current gets dissipated in the dump resistor. Adapted from [47].	18

11	Superconducting rectifier circuit with an inductive load. The superconducting switches diminish losses and operate the whole device in cryogenic conditions, where the color indicates that they are activated simultaneously. From [51].	19
12	Analogy between a transistor and a superconducting switch, indicating an open or closed state. The input control signal (red) is an electric current and a heat flow respectively. The main current to be switched is shown in blue and the resistance for each case is in green. A transistor has a small resistance in closed state, whereas a superconducting switch has zero resistance when it is closed.	21
13	Cross section of vertical tape stack configuration options for a ReBCO switch.	22
14	Single switch configuration, the ReBCO tapes are connected in parallel so the electric current (indicated with the arrowhead in blue for each ReBCO tape) flows in one direction.	22
15	Double switch configuration, the ReBCO tapes are connected in series, so the electric current flows in opposite directions, indicated by the arrowhead and arrowtail in blue for each ReBCO tape.	23
16	a) Experimental setup of the ReBCO based superconducting switch. Cross section of copper casing (orange) that comprises layers that make the superconducting switch, corresponding to Kapton (brown), ReBCO tape (red) and electric heater (gray). b) Cooling down of the setup is done with liquid nitrogen. From [51].	24
17	Test stand for the ReBCO switch. The ReBCO tapes are connected in the copper connections on the edges so the electric current flow along. The current I (blue) that runs through the superconductor is independent of the current I_{heater} (red) used to control the open and closed states of the ReBCO switch. From [51].	25
18	Lateral view schematic of a ReBCO tape, subjected to an etching process. Removing the copper and silver stabilizer layers increases considerably its total resistance, feature needed for a superconducting switch application. . .	26
19	Model in the simulation for the ReBCO tape, showing layers and approximate dimensions, which can be tuned to adjust the model to the experimental data.	29
20	Current sharing between superconducting and normal conducting layers. I is the total current that flows through the ReBCO tape.	30
21	Schematic for a Resistance vs Time plot, showing the time response parameters. A heat pulse is applied with a step current (orange), and there is an increase in the resistance due to surpassing the critical temperature (blue). The delay times are shown in purple, rising and falling times appear in green.	31
22	Simulation scenario for the current sharing between two superconducting lines, both of them in the single switch case. When one of them is quenched the current is redirected towards the other branch.	32
23	Current sharing between superconducting and normal conducting layers for two conducting lines. Each conducting line has its respective ReBCO tapes, hence its own superconducting and resistive material layers.	32

24	High current thermally activated ReBCO switch with 4 tapes. For a single switch configuration all the ReBCO tapes are connected in parallel, to increase the total current that can be conducted. For a double switch configuration, the ReBCO tapes for the bottom part are connected in parallel, as well as the ones for the top; and in the end, these top and bottom sections are connected in series.	34
25	Schematic for a thermal contact interlayer between two etched ReBCO tapes (note that there is still a thin silver layer remaining). The thin kapton layer serves as tuning value for the heat propagation between the ReBCO tapes for a non-uniform contact between them.	34
26	Temperature profile vs Vertical length, showing the effect of non-uniform thermal contact on temperature distribution for a 6 ReBCO tapes stack when a heat pulse is applied. The horizontal axis correspond to the length along the vertical axis in the tapestack, and the black vertical lines divide between the different material layers present in the tapestack. Note the drop in temperature between each ReBCO tape.	35
27	2D magnetic field strength in a point P generated by stacked ReBCO tapes. Each tape carries an electric current, that in joint effort create a self magnetic field, which diminishes the attainable critical current. From [32].	36
28	Temperature evolution, in function of time and the vertical dimension. Simulation run for a 2 ReBCO tape setup at 77 K, where a heat pulse is applied for 2 [s]. The dimension and time axis are on the horizontal plane, whereas the temperature is on the vertical axis.	38
29	Temperature evolution over time (left) and temperature profile at a given time (right) for 2 ReBCO tapes setup. These correspond to cuts in the temperature surface shown in the previous figure.	39
30	Overall resistance and time response, with 4 different curves for increasing number of ReBCO tapes connected in parallel. The top plot correspond to the decreased overall resistance when using more tapes, while in the bottom plot there is a slower switching time because of increasing the thermal resistance towards both the heat source and heat sink.	40
31	Time response for a heating pulse, for 2 etched ReBCO tapes in single switch configuration. The change of superconducting state can be observed as a rise in the resistance across the ReBCO tapes.	41
32	Current distribution vs Time, between conducting lines for two separate heat pulses in each conducting line. Observe that the electric current runs towards the opposite branch when its heater is activated.	42
33	Current distribution vs Time, between non-equal lines when activating each ReBCO switch separately. Voltage across the line (induced resistance times current) and Power losses produced vs Time, in lower plots. Note the effect in the second conducting line, produced by surpassing the critical current density.	43
34	2D magnetic field calculated for 4 tape pairs, single switch configuration at 50 K. The red lines indicate the direction of the magnetic field and the contour surfaces represent the total magnitude of the magnetic field along the 2D space.	44

35	Magnetic field magnitude and Critical current distribution vs Horizontal length, for 4 tape pairs. Single switch configuration at 50 K, showing the first 4 ReBCO tapes from bottom to top, since the values are symmetric respect the heater tape to the last 4 top ReBCO tapes.	45
36	2D magnetic field calculated for 4 tape pairs, double switch configuration at 50 K. The opposite direction of the current in the bottom and top sections change the distribution of the magnetic field, making its magnitude higher in the center of the tapestack and lower in its surroundings.	46
37	Resistance per unit length vs Heating power. Comparison between simulation and experimental data for a non-etched tape. A linear fit for the non-superconducting regions of the data is shown with straight lines (which correspond to the linear resistivity increase of the regular conducting materials in function of the temperature), along with the respective equation.	47
38	Top: Resistance per unit length vs Time. Bottom: Voltage vs Time. A time response comparison for 2 non-etched ReBCO tapes, at 77 K. There is a heat pulse produced by a 6 A current, and then the increase and decrease in temperature opens and closes the ReBCO switch.	48
39	Time response values vs Heater current both for simulation and experimental data. A comparison for non-etched tapes. Multiple heater electric currents where it can be roughly observed the same behavior for increasing heater currents.	49
40	Options for a 10 kA ReBCO switch, considering an operating temperature of 50 K and 12 mm etched ReBCO tapes. A) Single vertical tapestack. B) Double tapestack.	51

List of Tables

1	Commercially available superconducting materials and critical parameters of temperature and magnetic field. From [4].	4
2	Time response comparison between simulation and experimental data.	48
3	Time response for 10 kA ReBCO switch for both designs. The values presented are rounded.	51
4	Technical specs for 10 kA ReBCO switch for both designs. The values presented are rounded.	52

Glossary

A

AC Alternating Current. 13

C

CICC Cable in conduit conductor. 7

CORC Conductor On Round Core. 7, 13, 50

H

HTS High Temperature Superconductor. iii, 3–5, 7, 8, 12, 15, 16, 19, 58

L

LTS Low Temperature Superconductor. 3, 5–7, 12, 15, 16, 20, 55

M

MRI Magnetic Resonance Imaging. 3, 19

N

NMR Nuclear Magnetic Resonance. 3, 19

P

PCB Printed Circuit Board. 27

R

ReBCO Rare Earth Barium Copper Oxide. 3, 5, 6, 11–15, 20, 22, 23, 25–30, 33, 34, 36–38, 40–42, 44, 50–58

Acronyms

A

ATLAS A Toroidal LHC ApparatuS. 7

C

CCFE Culham Centre for Fusion Energy. 16

CERN European Organization for Nuclear Research. 4, 7, 13, 50

E

EURATOM European Atomic Energy Community. 16

H

HERA Hadron Electron Ring Accelerator. 3

I

IEC International Electrotechnical Commission. 11

L

LHC Large Hadron Collider. 4

M

MATLAB Matrix Laboratory. 7, 58

R

RHIC Relativistic Heavy Ion Collider. 3

U

UNK Accelerating and Storage Complex. 3

Abstract

A superconducting switch allows to redirect an electric current in a superconducting circuit, designed for this project by using High Temperature Superconductors. The available HTS conductors to date in form of tapes made of cuprate materials (ReBCO), and allow to operate in superconducting state at higher temperatures and magnetic fields than LTS materials.

The approach used for a high-current ReBCO switch is to stack multiple ReBCO tapes and connect them in parallel, in order to increase the total current that can be conducted. Then, with an electrical heater the temperature can be increased, and purposely make resistive the switch ("open" state), so the electric current flow towards a less resistive path.

A simulation model was developed for a thermally operated ReBCO switch, to predict its thermal and electric responses and test different operating conditions. Two designs for a 10 kA ReBCO switch are proposed, applicable to a superconducting rectifier project currently under development by the EP-ADO group at CERN.

Experimental measurements were performed to check and tune the model with the data obtained, from low current samples of a ReBCO switch setup developed by members of the workgroup. Further tests are required to scale a physical setup to 10 kA.

1 Introduction

1.1 Brief energy panorama

The world nowadays relies on electricity to sustain human endeavors ranging from transport, lighting, housing heating or industry applications. Different energy options exist to ultimately produce it, such as fossil fuel power plants, hydroelectric, solar, wind, geothermal, biomass or nuclear. They are based on different principles to ultimately convert them, such as e.g. thermal energy (combustion, nuclear reactions) or mechanical energy (hydro, wind). This means that in order to make an objective comparison among them it is needed to consider factors such as land area used per unit of energy produced, and fuel volume or weight consumed per unit of energy output [1].

It also depends on the geographical or environment characteristics, power requirements and even local available expertise to choose which energy source will fulfill more adequately the power requirements for a region. Additionally, political policies in different countries usually influence or favor which type of power generating source to be installed for economic or environmental reasons.

There are pros and cons for every type of energy source, so a well informed panorama of these factors can lead to an adequate energy mix that suits best the particular conditions for powering the grid [2]. As this text focuses on an application relevant to nuclear energy sources, in the following lines some relevant points will be introduced as a background. With the previously mentioned options, there are some advantages in making use of nuclear based systems as an energy source to produce electricity, such as:

- *No significant greenhouse gases produced*
Nuclear reactions don't rely in a chemical reaction (like the combustion process), the atoms themselves are interacting, and the waste produced is confined on-site. The greenhouse gas emissions are mainly produced during the construction process of a nuclear plant.
- *High energy density*
A nuclear reaction produces considerably more energy per mass unit than chemical reactions such as combustion, or by the conversion of energy that happens in wind and solar energy. Then, the required land area per unit of power produced is small compared to renewables such as wind and solar.
- *Weather independent operation*
Nuclear plants rely in on-site fuel consumed on demand, so it can function as a backload power source that is not affected by intermittency in power generation due to weather conditions.

The previous statements apply to the nuclear reactors that supply electricity today to the world grid, which are based in the reaction called nuclear fission. However, there are two types of nuclear reactions that happen in nature: fission and fusion.

Nuclear fission involves the splitting of heavy atoms into smaller elements, releasing energy

as a result. In comparison to fusion, it is relatively easy to produce fission in a controlled way, as the many nuclear reactors around the world relying in this reaction can testify. Unfortunately, the production of highly radioactive waste is a drawback for this technology. New nuclear reactor designs rely on using thorium or different updates to make more efficient the burning of the fuel, as well as to reduce the half-life of the radioactive waste. Proper management, treatment or disposal of the radioactive waste produced are important factors to use the technology in a safe manner and continue having this high energy density source that doesn't produce greenhouse gases as fossil fuels do.

Nuclear fusion is the source of energy of a star, where there is a balance between the gravitational attraction that holds its mass together and the expanding force due to the fusion of light elements and subsequent energy release from these reactions. In this scenario a constant energy output for millions of years is the result. And, although also relying on nuclear processes to generate energy, it produces lower grade radioactive waste than fission, which reach background radiation levels in a reasonable amount of time, so as not to become a problem for the future, due to the stockpiling of radioactive waste that can take thousands of years to decay [3], unless reprocessing of the waste is done to reduce this time frame.

However, achieving controlled nuclear fusion on earth is not a straightforward process, it has been tried by researchers around the world for the last 70 years or so. The challenge nowadays is to produce a machine with an energy gain factor greater than one, i.e. to produce more energy from the fusion reactions than the energy that is invested to produce these reactions in the first place. Succeeding in this endeavor will mean to have a nearly inexhaustible source of energy to contribute to the energy production to power mankind, as a high energy density alternative to fossil fuels, considering that the fuel, deuterium, is not region specific as fossil fuel deposits, since it can be extracted from water.

Some of the most successful designs so far for a nuclear fusion reactor are both the tokamak and the stellarator, that confine a plasma by magnetic fields in a toroidal configuration. Research is ongoing around the world to improve the overall performance of these types of machines, ranging from understanding of the plasma physics, control systems or plasma-wall interaction to extract and transform the thermal energy of the system. Magnetic confinement devices rely in high magnetic fields to contain the plasma in a vessel, so in order to achieve such fields the use of superconducting materials become a must, considering that they can reach current densities higher than the best conductors, such as copper or silver, which result in a higher electric current running through them that produce higher magnetic fields.

1.2 Superconductivity

Heike Kamerlingh Onnes in 1911 discovered superconductivity by measuring the resistivity of mercury at very low temperatures, cooling samples with liquid helium (which has a boiling point of about 4.2 K at atmospheric pressure) and observed that below a critical temperature the material loses all resistivity. Different superconducting materials have been found through the years since then [4], giving further insights in the phenomenon, although there is yet to find an accurate explanation of the reason why it happens, Bardeen–Cooper–Schrieffer (BCS) theory being the most accepted one.

Nevertheless, technology has been developed to exploit this material behavior, since it is more energy efficient using superconductors for high current applications. While a regular conductor such as copper would produce a high amount of heat by joule effect, which needs to be extracted by a cooling system, an equivalent rated superconducting device would produce no joule effect, and the energy investment in cooling the device is lower than an equivalent regular conductor case. In other words, regular conductors can produce high magnetic fields, but the cooling power required increases with the current running through the conductor, whereas for superconductor the only power needed is the one for cooling the device below its critical temperature, as long as the current remains below the critical current.

Superconductors have already been used commercially since the early 1960's in different industries. Compared to normal conductors they can carry electric current at considerably higher magnitudes with no Joule power dissipation.

In 1986 high-temperature superconductivity was discovered in cuprates [5]. Since then there has been significant research, and different varieties of materials with a critical temperature above liquid nitrogen have been described.

HTS to date have only been found in brittle materials, hence there is a fundamental limitation to make flexible wires as is the case with *LTS* such as *NbTi*. However, manufacturing techniques were developed starting in the 90s to make tapes of superconducting material with different layers, which can be bended slightly while mostly conserving their superconducting properties, along with the capacity to manufacture them in industrial scale, which allows the production of both cables and coils with them.

Different superconductor cable designs have been proposed to handle high currents and high magnetic fields. For this reason there are factors taken into account such as reduction of total material used for the tapes, loss optimization or maximizing the current density.

Low Temperature Superconductors (*LTS*) such as niobium–titanium (*NbTi*) and niobium–tin (*Nb₃Sn*) are the workhorses of superconductor technology, however they need to be cooled at liquid helium temperature at about 4.2 K or lower, depending on the application. High Temperature Superconductors (*HTS*), nowadays mostly ReBaCuO-based (Rare Earth Barium Copper Oxide or *ReBCO*), can potentially work at temperatures closer to liquid nitrogen (boiling point at about 77 K, operation at about 30-50 K). It is considerably cheaper as a coolant and widely available, while increasing the attainable magnetic fields and current densities compared to *LTS* [6].

Magnetic Resonance Imaging (*MRI*) and Nuclear Magnetic Resonance (*NMR*), in the medical industry, are among the largest commercial applications of superconductivity, while there are some emerging applications such as levitating systems for transportation; lossless power distribution systems for the electric grid; and lighter, smaller and more energy efficient electric or electronic devices. Superconducting magnets are also used in large physics experiments related to plasma and particle physics in research laboratories around the world, both for magnetic confinement and highly sensitive detection equipment like the Relativistic Heavy Ion Collider (RHIC) in the United States, the Accelerating and Storage Complex (UNK) project in Russia, the electron–proton collider Hadron Electron Ring Accelerator (HERA) in

Germany, and most recently the Large Hadron Collider (LHC) at the European Organization for Nuclear Research (CERN) [7].

A summary of commercially available superconducting materials and their critical parameters is shown in Table 1 [8–14]:

material	$T_c(0)$ / K	$B_{c2}(0)$ / T	application area
NbTi	9.3	12 - 15	medium field: magnets up to 9 T
Nb ₃ Sn	18.3	25 - 29	high field: magnets up to 15 - 20 T
BSCCO 2212	95	175 - 225	highest field: inserts for magnets above 20 T
BSCCO 2223	107	107	medium field: e.g. power cables and current leads
ReBCO	92 - 95	120 - 250	highest field: inserts for magnets above 20 T
MgB ₂	35 - 39	14 - 40	low to medium field: e.g. wiring in satellites

Table 1: Commercially available superconducting materials and critical parameters of temperature and magnetic field. From [4].

1.3 Relevance of Superconductivity in Nuclear Fusion

In the case of nuclear fusion research, high magnetic fields are required in order to confine the plasma, and the development and implementation of *HTS* magnets will allow to improve the performance of the new generation of fusion experiments, increasing the attainable magnetic field that results in a better confinement of the plasma inside the vessel, and consequently impacting directly on the fusion reactions produced.

In a tokamak and other types of toroidal magnetic confinement devices, an important parameter to describe the plasma is the toroidal beta (β_T), defined as the ratio of the kinetic plasma pressure to the magnetic pressure:

$$\beta_T = \frac{\bar{p}}{\frac{B_0^2}{2\mu_0}}$$

with \bar{p} the volume averaged plasma pressure and B_0 the toroidal magnetic field on the plasma axis, defined by the torus' major radius R_0 .

The power density ($\frac{P_f}{V_p}$, fusion power over volume) scales with the square of the kinetic pressure, so replacing the previous equation for the definition of toroidal beta this results in:

$$\frac{P_f}{V_p} \propto \bar{p}^2$$

$$P_f \propto \beta_T^2 B_0^4 V_p$$

This proportionality highlights the advantage of increasing the magnetic field in a fusion device because of this fourth power dependence (considering a constant β_T), i.e. obtaining a 16 times multiplication of the fusion energy produced by duplicating the magnetic field, or reducing the volume of the machine for the same power output, with its associated economic benefit [15, 16]. It is also worth to note the linear increase in fusion power with the volume of the machine, that although for one it increases the total cost and lead an increase in manufacture difficulty, on the other hand it has advantages such as neutron shielding from the fusion reactions and higher area and volume to exhaust heat and neutron loads.

In order to produce a high magnetic field, a high electric current runs through the superconducting coils of the fusion reactor. If there is an unexpected loss of superconductivity, the high stored energy needs to be dissipated in an external resistor in order not to damage the coil. Additionally, it is possible to implement devices that can slowly charge or discharge a superconducting coil without needing a high current source. These applications, quench protection and superconducting rectifier respectively, will be explained in the next chapter, and make use of the so called superconducting switch.

1.4 Project Definition and Research Question

A superconducting switch is a device that allows to redirect the current in a superconducting circuit, e.g. in superconducting magnet applications. They are based on a change of resistivity to change its state: high resistivity ("open" state) and zero resistivity ("closed" state), which can be controlled by modifying its parameters, so threshold values of either temperature (T), magnetic field (B) or current density (j) are surpassed, after which the material loses superconductivity and enters to a normal conducting state.

The use of *HTS* materials for a superconducting switch is expected to provide a better performance than a *LTS* based one, because of a wider operational window. *HTS* conductors commercially available come in the form of planar tapes of superconducting and stabilizer layers, technology used for developing the *HTS* switch (from now on referred as *ReBCO* switch) in this project, specifically making use of *ReBCO* tapes.

Using a heat source to control the temperature (and hence the superconducting state) is also the chosen approach for this project because of the simplicity in its implementation. Then a thermally activated superconducting switch is defined, considering that a successful design was tested before with *LTS* technology [17]. There are also tests for low current *HTS* switches operated by inducing a high magnetic field, but require additional parts and considerations [18].

Superconducting coils in fusion devices have currents in the order of one to tens of kilo amperes, to then produce the desired magnetic fields. So, as a goal for this project, a 10 kA *ReBCO* switch is the design objective, being rated in a magnitude of electric current relevant for superconducting magnets used both in nuclear fusion and other applications. The reason is that the current that flows through the superconducting coil also flows through the superconducting switch, i.e. they are connected in series in a superconducting circuit.

Stacking *ReBCO* tapes is the simplest approach for a high current conducting line, so they

are connected in parallel to increase the current carrying capacity, so in joint effort they conduct the total superconducting current flowing through the *ReBCO* switch. The heat source for the thermal control is produced by means of a resistive steel strip in close contact with the superconducting tapes, and by running an electric current through it, the adjacent *ReBCO* tapes can be warmed up to control the superconducting state. Otherwise, different high current *ReBCO* cable designs exist, such as CORC or Roebel, which are an alternate option for conducting the current against the parallel *ReBCO* tapes option.

Taking into account that the critical temperature of *ReBCO* tapes is around 92 K, it is possible to make tests at liquid nitrogen temperature, which reduces the costs to make experiments as compared with the higher cost liquid helium required for *LTS*.

Regarding the operating temperature, it is necessary to investigate working at lower temperatures than that of liquid nitrogen (77 K), that will allow reducing the number of *ReBCO* tapes but also have impact on the switching speed of the device, due to longer heating and cooling down times. On the other hand, stacking many *ReBCO* tapes in a higher operating temperature scenario, will result in a slower heat propagation, which also affects the speed of the device.

The presence of a magnetic field, external or self induced for a high current conductor, reduces the critical current density in a *ReBCO* tape, so there is a slower than linear increase in the critical current density when increasing the number of parallel *ReBCO* tapes. This depends on the geometric configuration of the tapestack, which influences the magnitude of the magnetic field along the space around the *ReBCO* tapes.

The heat propagation depends on the different layers of materials involved, and particularly for the *ReBCO* tapes, since they are on their own composed of different materials. A simplified model of the *ReBCO* tape is also necessary, which then also influences the overall thermal response of the tapestack.

The dimension of the *ReBCO* switch in the longitudinal direction, which is also the length of the *ReBCO* tapes used, is a factor to be explored, since it has a direct influence on the overall resistivity, total cost and power consumption of the device.

As it can be seen, there are a variety of factors that have ultimately influence on the technical specifications of the thermally activated *ReBCO* switch. It is then convenient to have a simulation model where the thermal and electrical behavior can be investigated, and different tape stacks configurations can be tested, considering *ReBCO* tapes are expensive, and experimental testing is time consuming.

Then, determining a working configuration with the model will allow to guide the experimental testing faster towards a design that can comply with the desired specifications. A physical setup for low current was already working by the time this project started, and the model intends to contribute and guide the tests done towards a high current configuration.

So, the following research question is stated, taking into account the previous factors, in order to develop a design for a high current application:

Can a 10 kA thermally activated superconducting switch be developed with ReBCO tapes technology, and a switching frequency of 1 Hz?

The switching frequency, based on the speed response of previous *LTS* designs, is desired to be of the same magnitude. The operating temperature of the device is expected to be lower than that of liquid nitrogen. It is then necessary to consider some additional, closely related factors:

1. *What is an adequate temperature for the ReBCO switch to operate?*
2. *Is the influence of magnetic field produced by the high current manageable in a multiple ReBCO tapes scenario?*
3. *Are parallel connected ReBCO tapes sufficient or is it necessary to opt for an alternate high current ReBCO cable?*

The simulation model is developed using the *MATLAB* platform, considering that the group already has some libraries regarding the computation of the physical properties of the material, the calculation of the 2D magnetic field produced by a conductor with rectangular cross section, as hardware and software developed to extract the data produced from the experimental setup.

This project was developed within the ATLAS research and development team at CERN, Experimental Physics Department - ATLAS Detector Operation Group. The group has expertise in developing applied superconducting technology, both for particle accelerators as for nuclear fusion applications.

This expertise ranges from current leads, cryogenic systems, and superconducting magnets with *LTS* technology. Currently tests towards *HTS* cables and magnets are being developed in the group, making use of the *CORC* cable design, which comprise high current cables such as *CORC-CICC* as well as *CORC* based solenoids [19–22]. The present project then intends to develop a design for a *HTS* switch, which is relevant for being part of a planned *HTS* superconducting rectifier, whose elements are currently being developed as parallel projects by other members of the research group.

2 Superconductivity Technology Progress

In this chapter relevant concepts for superconductivity are introduced, along with the current state of *HTS* technology, including high current cables, switches and their application in different technology areas.

2.1 Superconductivity concepts

2.1.1 Type I and Type II Superconductors

There are two types of superconducting materials, classified as Type I and Type II, their difference lies in how an external magnetic field penetrates into the material and affects the superconductivity state, considering that the material is below the critical temperature.

A superconductor at very low field behaves as a perfect diamagnetic material, known as the Meissner effect, where external magnetic fields are completely excluded from the interior of the material. However there is a critical magnetic field B_c where this effect is surpassed, and superconducting state is lost [23]. Depending if the superconductor is Type I or Type II, the transition to normal conducting state is respectively either sharp or gradual.

In Type I superconductors, considering that the material is below its critical temperature, and after the critical magnetic field is surpassed, the magnetic field completely penetrates the material and the resistance returns. Usually the maximum field in these superconductors is less than 0.1 [T], and an electric current can only flow in a thin layer at the surface of the material, usually in a few micrometers depth. These limitations make Type I superconductors not useful for wire and cable applications. Most elemental superconductors are Type I superconductors (with some exceptions such as Nb, V and Mo which are Type II).

In Type II superconductors, there is a transition zone after a lower critical magnetic field B_{c1} is surpassed, and the magnetic field penetrates the material in the form of discrete flux lines. This produces a mixed state with superconducting and normal regions inside the sample. The superconductivity is only destroyed completely and the normal resistance state reached when the applied magnetic field is larger than an upper critical field B_{c2} . Most alloys and compounds are Type II superconductors, for which they are the ones that are usable to fabricate wires and cables for high current applications [24, 25].

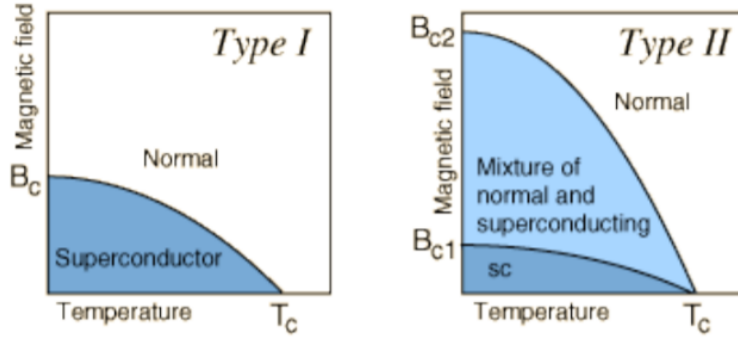


Figure 1: Diagram B vs T for Type I and Type II superconductors, critical values B_c and T_c are codependent limits to the transition to the normal conducting state. There's a sharp state change in Type I superconductors, and a transition region for Type II. From [26].

2.1.2 Resistivity and Critical Temperature

To achieve superconductivity in a material it's necessary to cool it down below its critical temperature, a value that depends on the composition of the material. After getting past this value the superconducting phenomenon is observed, that for Type II superconductors occurs in a transition phase in a small temperature window, as shown in Figure 2:

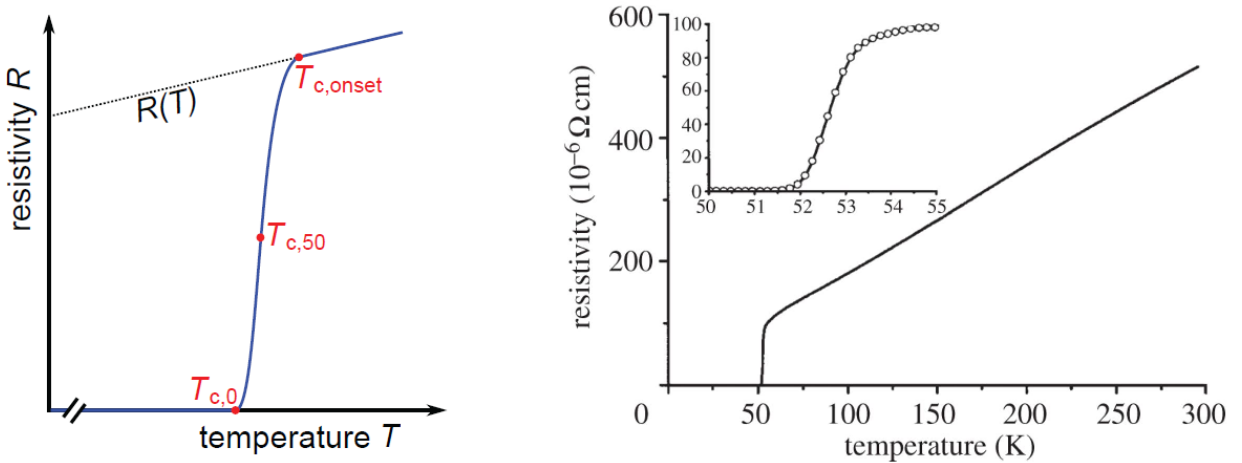


Figure 2: Schematic for Resistivity vs Temperature, showing the transition from superconducting to normal conducting states when exceeding the critical temperature of a Type II superconductor. Left: Mixed state between $T_{c,0}$ and $T_{c,onset}$, while getting to a temperature lower than $T_{c,0}$ makes virtually all resistance in the material to disappear [4]. Right: Resistivity vs Temperature for a LaSrCuO material, showing zoom-in in the transition temperature window of about 2 K between superconducting and normal conducting states [27].

An external magnetic field, as well as a high pressure, can both modify the value of this critical temperature. On the following section is explained how to further determine the parameters than finally set the electric current that can be conducted in a superconducting material.

2.1.3 Operating in superconducting conditions

As seen so far, there is an interdependency in the temperature, magnetic field and current density of a superconductor. These interconnected parameters have critical values, that define a threshold above which the superconductivity is lost. This situation is shown in Figure 3, in the so called critical surface.

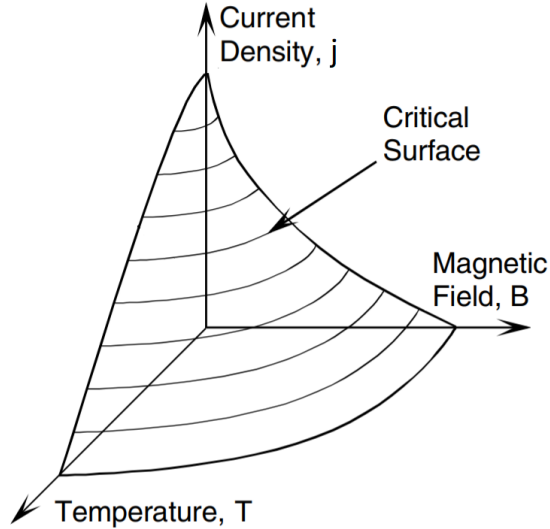


Figure 3: Schematic for the critical surface in a Type II superconducting material, where T, B and j are interdependent values. To operate in superconducting state it is necessary to stay below the critical surface. Any point of the critical value correspond then to three interdependent values of T_c, B_{c2} and j_c . Adapted from [5].

Having a high current produces a high magnetic field, so a temperature margin from the critical surface is required to have a good performance with lower quench risk. For this reason, the lower the operating temperature, the more stable the device, since the system is more robust to fluctuations in the operating values.

Speaking of a superconducting line, application of interest for this project, what is relevant is the current density achievable in it.

The first step is to be at a temperature T_0 lower than the critical temperature of the material and zero magnetic field, at this condition the material by itself has a defined critical current density j_c . But a magnetic field B_0 , either external or self induced by a current running through the material, produces a reduction in the critical current density at the sample, for which we can state that the current density is a function of the magnetic field and temperature:

$$j_c = f(T_0, B_0)$$

As mentioned, it is also necessary to have a margin in the working values with respect to the critical surface, to then have a stable operation and small deviations in the operating values don't risk losing the superconducting state. This is exemplified in Figure 4:

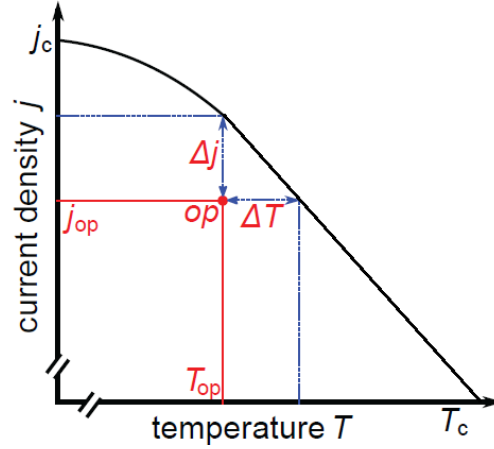


Figure 4: Schematic of Current density vs Temperature, for the operating point of a superconductor at a fixed magnetic field value B_{op} . Δj and ΔT are the safety margins from the critical surface, shown here as a 2D cut with the line that joins T_c and j_c , which is part of the critical surface. From [4].

2.1.4 Power Law Equation

When a Type II superconducting material is close to its critical temperature, considering it is being warmed up, it starts to develop a resistance. Additionally, considering that there is a current running through it, this results in a measurable voltage, which can be expressed as an electric field following the so called "Power Law" shown in Equation 1:

$$E = E_0 \left(\frac{j_{sc}}{j_c} \right)^n \quad (1)$$

The equation describes the electric field in the superconductor, where J_{sc} is the current density of the superconducting part, J_c is the critical current density of the *ReBCO*, n is a temperature dependent factor that increases proportionally with the temperature, and E_0 is the electric field criterion [28].

The electric field criterion is defined by the IEC International Standard 61788-1 as $1 \left[\frac{\mu V}{cm} \right]$, which is a set value often used for defining critical current density in superconductors [29]. In Figure 5 it is shown the definition of the critical current density, which is a value with a magnitude big enough to be measurable, but small so it doesn't cause a thermal runaway with the electric current that is being conducted because of joule effect.

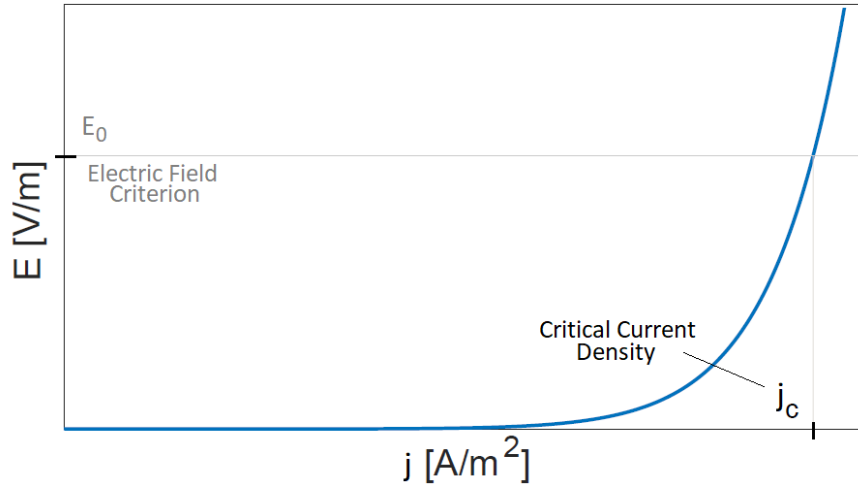


Figure 5: Schematic for Electric field vs Current density, to show the definition of the critical current density j_c in a superconductor, as the value where the electric field criterion E_0 is reached. Adapted from [30].

2.2 HTS Tapes

Fabricating a *HTS* tape is not a straightforward process, due to the brittleness of the materials commercially available now for *HTS* conductors, this when compared to the extrusion process that can be done for a ductile *LTS* material such as *NbTi*, which allow to have long and flexible wires.

ReBCO based *HTS* tapes are one of the commercially available options, used as the superconducting tapes in this project. The "Rare-Earth" part of *ReBCO* materials can be composed of any of the 15 elements in the lanthanide family of the periodic table, including scandium and yttrium. Is this last element, Yttrium (Y), the one that's widely used in commercially available tapes, along with Gadolinium (Gd).

Conducting tapes can be fabricated by atomic deposition processes in order to create a layered structure, which contains both superconducting and normal conducting elements, as *LTS* materials do, for thermal and electrical integrity. A substrate layer, usually a stainless steel alloy, provides the mechanical structure to the tape. Figure 6 shows a schematic of different layers that can be in a *ReBCO* tape:

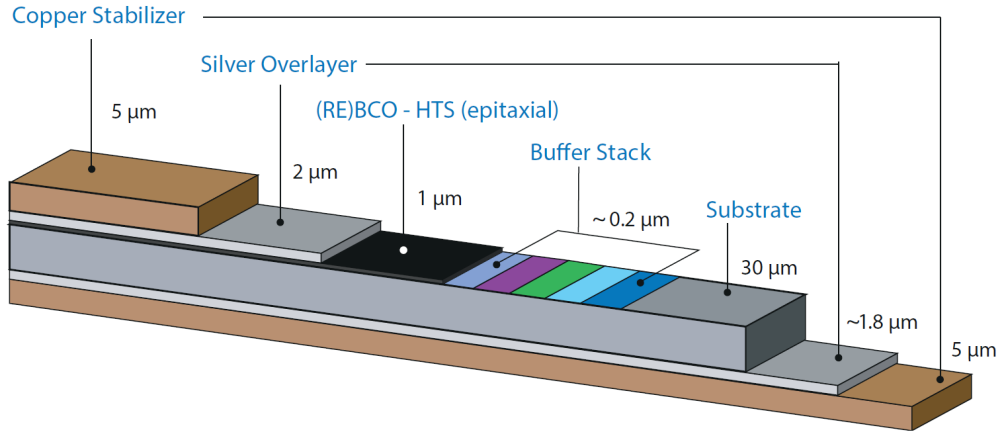


Figure 6: Schematic for a ReBCO tape. Note that the superconductor material is only a small fraction of the total thickness, and also includes regular conductor stabilizer layers. Design by SuperPower Inc. From [31].

The normal conducting layers serve as a conducting path for the current in case the superconductivity is lost, for which the resistance of the superconductor above its critical temperature is typically higher than the one of good conductors (such as copper or silver). These good conductor layers then help to protect the *ReBCO* layer in case of a quench of the tape, conducting the current that otherwise would be dissipated in the *ReBCO* layer.

2.3 High current ReBCO Cables

Different proposals for high current cables based on *ReBCO* tapes have been developed, in this section there are mentioned some of the options available, as well as a more in-depth description for the cable, linked with applied superconductivity projects developed at CERN.

Since *ReBCO* tapes are the format available at the moment for developing relevant technology, all the following concepts consider making different kinds of arrangements with the tapes in order to produce a high current superconducting cable.

All the following cable concepts are designed to operate at high electric currents while allowing some bending. Each of them specializes in trying to solve the problems that affect the scaling towards a high current *ReBCO* cable, such as *AC* losses, current degradation due to bending or the magnetic field effect.

Further testing can determine its adequacy depending on the type of application in mind, considering fusion, health care, or experimental physics relevant devices.

2.3.1 ReBCO based Cable Concepts

A brief overview of some *ReBCO* cable proposals is presented, which are options in order to produce a high current cable, considering that they can be used as an alternative approach towards a *ReBCO* switch respect with a simple tape stacking.

- Twisted stacked-tape conductor (TSTC) [32]

Developed at the Massachusetts Institute of Technology and Tufts University. It consists in stacking the *ReBCO* tapes and then twisting them along the stack axis.

- ReBCO Roebel cable [33]
Manufactured first by members of Karlsruhe Institute of Technology and the Slovak Academy of Sciences. Originally for copper cables, consist on segmenting and intertwining together strands of *ReBCO* tapes. Feature low AC losses.
- Round twisted stacked conductor [34]
Tested at the École Polytechnique Fédérale de Lausanne and the Paul Scherrer Institute. Consists on stacks of *ReBCO* tapes surrounded by a circular copper casing.
- ReBCO cable-in-conduit conductor [35]
Project developed at the ENEA Superconducting Laboratory. Conformed by a cylindrical core with helical slots, where *ReBCO* tapes are wound around.
- Stacked tapes assembled in rigid structure conductor [36]
Joint project from the Toki Graduate University for Advanced Studies, National Institute for Fusion Science and Tohoku University. Stacked *ReBCO* tapes in a square copper stabilizer with support structure, achieving successful tests at 100 [kA].
- HTS-CrossConductor (HTS-CroCo) [37]
Developed at Karlsruhe Institute of Technology. Stacked *ReBCO* tapes while using different tape widths to maximize the cross sectional area and current density, surrounded by a circular casing.

In Figure 7 are shown the aforementioned cable concepts.

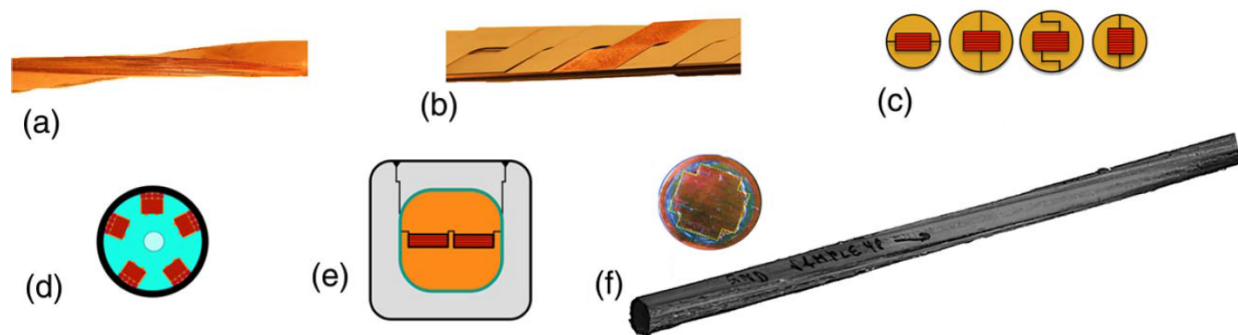


Figure 7: Different types of proposed ReBCO cables by different research groups. (a) Twisted stacked-tape conductor (TSTC). (b) Roebel cable. (c) Round twisted stacked conductor. (d) ReBCO cable-in-conduit conductor. (e) Stacked tapes assembled in rigid structure conductor. (f) HTS-CrossConductor (HTS-CroCo). Adapted from [38].

2.3.2 CORC-type High Current ReBCO Cable

The Conductor on Round Core, as the previously mentioned concepts, is designed to operate at high current in high magnetic field applications. The cabling approach consists of the helical winding of *ReBCO* tapes on a round core. The transposition of the tapes within

each layer of the cable significantly reduces the cable magnetization while the coaxial and mechanically decoupled arrangement of the tapes enables them to slide when the cable is bent, making them particularly flexible, achieved by leaving gaps between the *ReBCO* tapes that give room to some sliding of the *ReBCO* tapes between them, that make the cable relatively flexible to allow some bending [19].

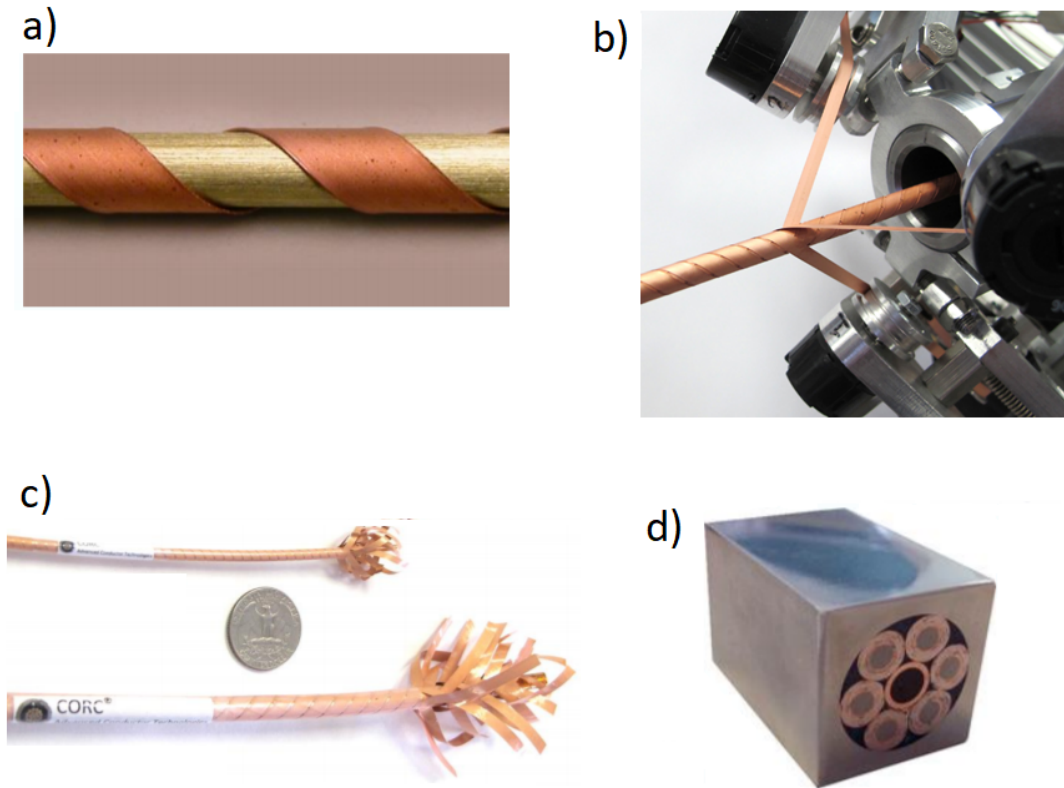


Figure 8: CORC cable production: a) ReBCO tape wound in round conductor, b) Winding of multiple ReBCO tapes in round conductor, c) Different diameter CORC cables, d) CORC-CICC for high current applications. Adapted from [20].

Various configurations of CORC cables have been tested to improve their performance for high-current and high-field applications, by a joint collaboration between CERN, Advance Conductor Technologies LLC and University of Twente. Research including both CORC wires and magnets, as well as CORC-CICC for higher currents, are relevant for nuclear fusion applications [20].

2.4 Status of HTS Technology for Nuclear Fusion Applications

An advantage that comes with the use of *HTS* is the wider window of temperatures for which the systems can be operated. In the case of nuclear fusion application, this allows the development of modular coils that have demountable joints, where the excess heat produced by them can be extracted while still operating in the superconducting state. Designs of magnets with demountable joints for tokamak and heliotron reactors were proposed in the 1980s, however, the heat generated by the joints for *LTS* temperatures (around 4K) was considered

too high to be exhausted while maintaining the system below the critical temperature, which would then result in reducing the stability of the magnets.

It's important to keep in mind that although the resistance of the joint is at the $n\Omega$ level, the additional generated heat still has to be extracted by the cooling system. It is expected that this will account for a few percent extra of the total cryogenic load in a tokamak using this kind of modular coils, which is considered to be still affordable [39].

The advantage of having coils with demountable joints is that it would enable modular construction of very large or complex superconducting magnets. This facilitates the reactor maintenance operations by improving access to its interior and disassembling of the machine; hence increasing the total availability of a fusion reactor by reducing the required time for maintenance campaigns.

Different proposals regarding modular coils have been published for fusion devices making use of high temperature superconducting coils, including helical coils as they are used in the Large Helical Device from the National Institute for Fusion Science in Japan [40], as well as coils for tokamak designs such as ARIES and ARC from the Massachusetts Institute of Technology in the US [41, 42]. The construction of modular systems becomes convenient both for building and maintenance purposes, particularly considering the increasing size of fusion devices such as ITER.

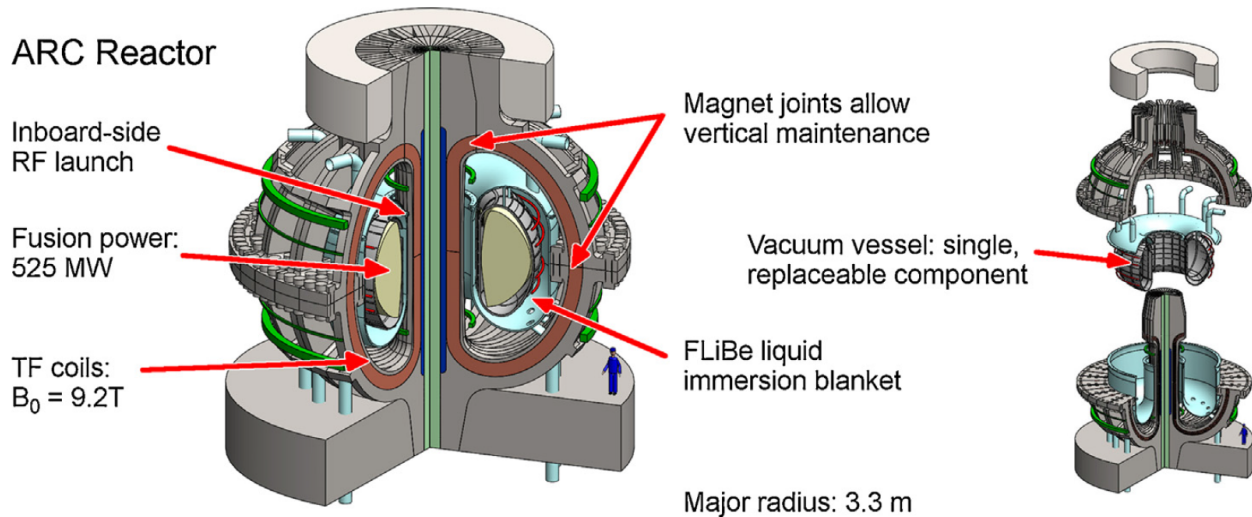


Figure 9: ARC reactor, featuring modular *HTS* coils, a liquid blanket, and vertical assembly for facilitating access and maintenance, with a major radius of 3.3 [m]. From [42].

Furthermore, in the last years it starts to become feasible, due to the increase in availability and some decrease in cost of *HTS* materials (still expected to be maintained at a relatively high value because of the use of expensive materials such as silver), to design reactors that make use of this technology instead of the classical work horse *LTS* from which all devices are built nowadays. For example, research done by Durham University and EURATOM and CCFE, for comparing the cost of electricity of a nuclear fusion power plant with both *LTS* and *HTS*. Assumptions given in the technological capabilities of *HTS*, it seems feasible

to reduce the size and cost of the machine, due to an improved confinement of the plasma derived from a higher magnetic field, as well as working with higher operating temperatures to eliminate the need of using the expensive liquid helium as a coolant [43].

2.5 Superconducting Switch Applications

A superconductor element changes from the superconducting state (zero resistivity) to the normal state (resistive state) when temperature, current density or magnetic field exceed a certain critical value. As a result, by modifying any of these parameters at will, the resistivity of a device can be controlled to change the direction of a current in a superconducting circuit. Hence, a superconducting switch is created, by provoking or nullifying on demand its resistivity.

The easiest approach is using the temperature as the control parameter, by heating segments in a superconducting circuit [17]. There are designs that use a magnetic field as well to control the superconducting state [18], and although in principle increasing the current density can also change its state, this last approach is not preferable since the current that is wanted to be dissipated or redirected will increase and be more potentially damaging for the system, although some designs have been developed with a current-stimulated quench approach for low current devices [44].

In the next sections some applications of superconducting switches are mentioned.

2.5.1 Quench protection circuits

A superconducting line can accidentally lose the superconductivity state (quench) as a result of surpassing any of their critical values. A cable for magnet applications use wire made from superconducting filaments embedded in a normal conductor (like copper), if there is loss of superconductivity in the filaments the current is transferred from the superconductor to the normal conductor, which protects the superconductor but also results in ohmic heating.

Depending on the design of the coil and cooling system, a region of a magnet that has quenched may or may not recover and return to the superconducting state. In the latter case, continuous current flow leads to continuous heating and potentially an irreversible damage to the magnet. Depending on the energy stored in the magnet, it might be sufficient for the energy to be dissipated in the magnet cold mass without excessive temperature rise, usually achieved by activating heaters to quench the entire magnet and dissipating uniformly the stored energy. But specially for magnets in nuclear fusion applications the stored energy is high, so quench protection requires to discharge this energy in external resistors [45].

Having safety measures to avoid the malfunction and damage of the superconducting coils on a fusion reactor is fundamental, considering that their cost can be over 30 percent of the total cost of the machine [46]. The system needs to be able to sustain the current that circulates in steady state in the superconducting coil, while effectively cutting the current flow if a quench is detected, so the current gets mainly dissipated in an external dump resistor. On the other hand, a superconducting rectifier has benefits both in reducing the cost and heat load to the cold mass, respect to a conventional power supply.

A superconducting switch can operate in a quench protection circuit for a superconducting coil, on the basis that its resistivity can be modified as function of any of its threshold factors. An example is shown in Figure 10, for a persistent mode circuit.

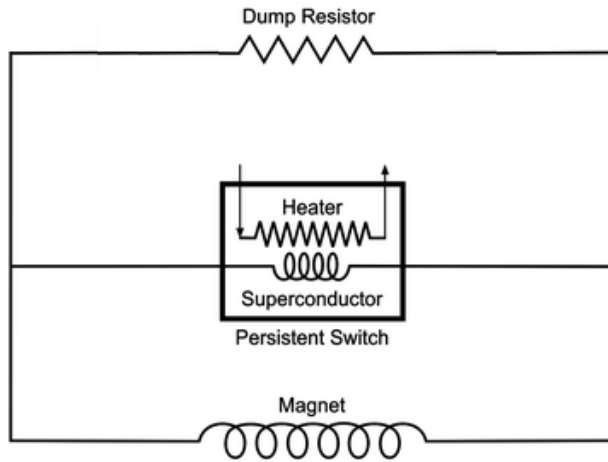


Figure 10: Schematic for a basic persistent mode, quench protection circuit with superconductor switch. The switch in normal operation is cold (hence superconducting), so the current flows unimpeded through it. When the switch is heated up its resistance increases, and the electric current gets dissipated in the dump resistor. Adapted from [47].

For this reason, superconducting switches can also be used to increment the operation time in the so-called persistent mode. Considering that once a current flows in a superconducting coil joined by a superconducting switch (since the resistivity is zero), no power is needed to maintain that current (no ohmic loss). So the current source can be turned off and the current will keep flowing virtually indefinitely. The advantages of operating in persistent mode are no power consumption from the power source after charging the coil, a drastically reduced heat load to the cold mass and a highly stable magnetic field.

The most common design is by connecting a superconducting wire that is resistive when warm across the terminals of the coil. A small heater is placed in close proximity to the wire. When the coil is being charged, the heater is turned on so the short across the magnet terminals is driven above its critical temperature and effectively becomes a resistor across the magnet terminals. When the appropriate operating current in the magnet is reached, the heater is shut off and the persistent switch is allowed to cool until it becomes superconducting, closing the superconducting loop [48].

2.5.2 Superconducting Rectifier

Compared to normal conductors, the current carrying capacity of superconducting wires, tapes and cables allows to increase the magnetic field magnitude in superconducting coils, while reducing the size and total power consumption. Their application is influenced by the heat leak from the environment, which is directly related to the capacity of the cryogenic system that needs to be installed in order to keep the superconductor below its critical

temperature. Reduction of heat leaks translates as a higher efficiency and smaller cooling systems, desirable for commercial applications.

In superconducting coils, where a current needs to be injected, it can either be done with conventional power supplies or with a superconducting rectifier (also called flux pump), which is a cryogenic power supply for inductive loads. Because the device works in the same environment as the superconducting load (i.e. alongside a superconducting coil, at the same cryogenic temperatures), the heat leak and ohmic dissipation losses in the case of high current injection and heat leaks from room temperature to the cryogenic space are highly diminished, whereas the power transfer efficiency can be $>95\%$ [49], as well as reducing the energy cost respect to conventional power supply for currents above some hundreds of amperes [50].

The device then is able to convert an alternating electric current with small amplitude into a large step-wise increasing superconducting current. It can therefore be applied as a current supply for superconducting loads that require large operating currents. The advantages are first, because for high currents a superconducting rectifier system is less expensive than a conventional power supply; and second the mentioned heat leak is considerably reduced [17].

A circuit for a superconducting rectifier is shown in Figure 11, with primary (L_p) and secondary coil (L_s) of the transformer, four thermally activated superconducting switches (S_1, S_2 and S_3, S_4) and an inductive load (L).

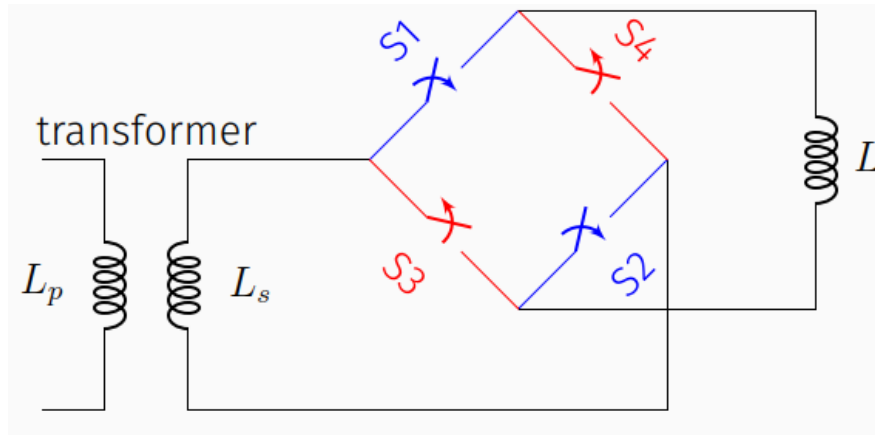


Figure 11: Superconducting rectifier circuit with an inductive load. The superconducting switches diminish losses and operate the whole device in cryogenic conditions, where the color indicates that they are activated simultaneously. From [51].

Superconducting rectifiers can be used not only for injecting current but also for compensating the current loss over time due to the decay caused by operation or resistive segments (e.g. resistive joints or defects in the material).

For these reasons they are applicable in nuclear fusion superconducting coils, considering that there are already some developments to use these devices in the coming generation of superconducting coils made with *HTS* materials [52]. Other areas that can benefit with this technology include magnet systems for particle accelerator devices [53], *MRI* and *NMR* coils in the medical field [54], and superconducting magnetic energy storage [55, 56].

3 Basis to build a ReBCO based superconducting switch

In order to predict the behavior of the *ReBCO* switch, a thermal/electric computational model was developed for this purpose. Additional considerations are necessary to pass from a low current to a high current model, namely the non-negligible magnetic field in the tape stacks and different rates for heat propagation due to increasing the number of layers in the tape stacks.

Developing a computational model has then the purpose of having a tested configuration that can work with the designed specifications, to reduce time in testing of different physical setups, so as to build one as an educated guess, having a reasonable certainty of its success due to all the variables involved; as well as reducing the cost of the system, since the market price of *ReBCO* tapes is still fairly high compared with *LTS* wires.

3.1 Superconducting switch principle

It's worthy to note that the superconducting switch for the present project has a solid state operation, i.e. there is no physical movement involved in the "open" or "closed" states. In the "open" state the switch has a high resistance, whereas in the "closed" state it is superconducting. This can be explained making an analogy with a transistor, taking into account that, when the superconducting switch is "open" its resistance is large, and it's zero when "closed", whereas in a transistor there is a finite resistance for the "closed" state.

The control signal that "closes" the transistor is the electric current that is applied to its base pin, whereas for the superconducting switch a heat input causes a temperature increase that "opens" the switch (critical temperature is surpassed and the path becomes resistive). When the electric current in the base pin is zero, the transistor acts as an "open" switch, and the superconducting switch is "closed" when there is no heat input. This situation is shown in Figure 12.

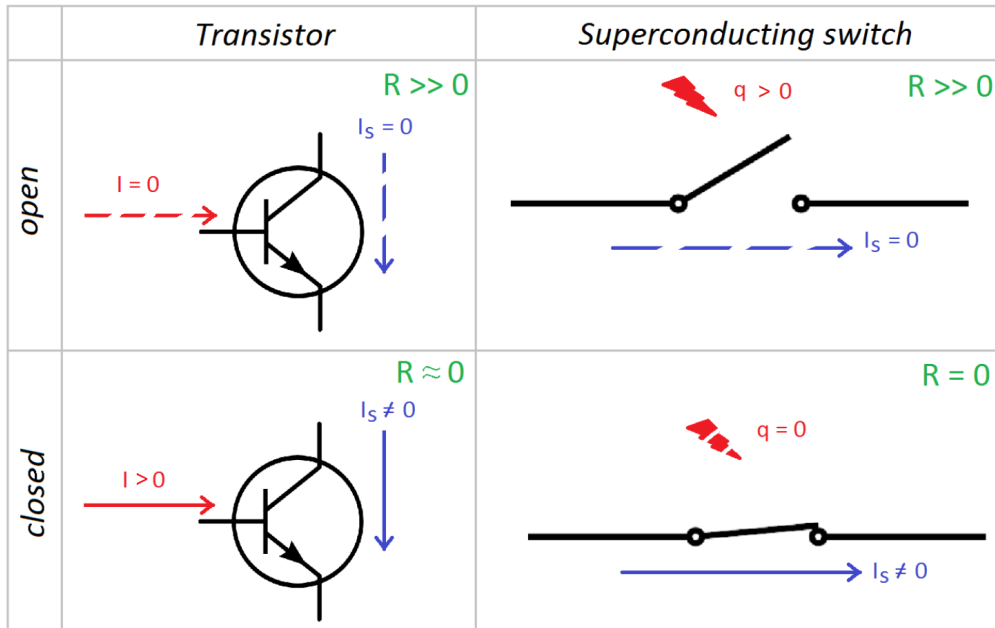


Figure 12: Analogy between a transistor and a superconducting switch, indicating an open or closed state. The input control signal (red) is an electric current and a heat flow respectively. The main current to be switched is shown in blue and the resistance for each case is in green. A transistor has a small resistance in closed state, whereas a superconducting switch has zero resistance when it is closed.

3.2 Superconducting switch with ReBCO tapes

The design for a superconducting switch consists of a tape stack of different layers:

- *ReBCO tapes*
They carry the main electric current through the device.
- *Electric heater*
Resistive strip made of a steel alloy (hastelloy) used for heating the device by running an electric current through it (so its temperature increases due to Joule effect).
- *Kapton*
They provide electrical insulation between the different layers, so the current used for the heater won't flow to the superconducting tapes, or the current from the tapes don't flow to the copper edges.

The copper edges function as heat sinks that remain at the cryogenic operating temperature, which are part of a copper block big enough to maintain its low temperature during operation. Two configurations for this purpose were considered, shown in Figure 13:

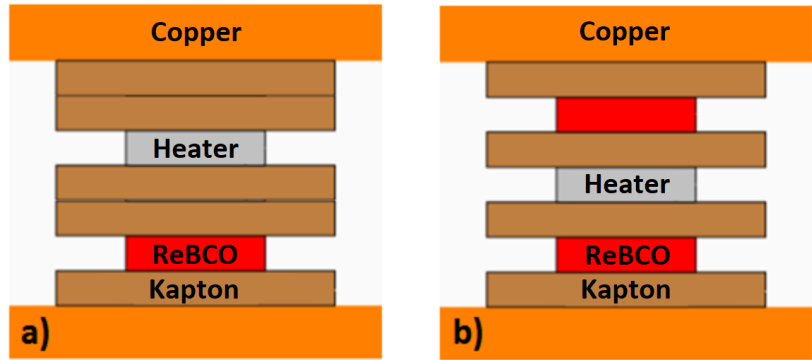


Figure 13: Cross section of vertical tape stack configuration options for a ReBCO switch.

From the tape stack 13.a) a single *ReBCO* tape was considered, with a double layer of Kapton to reduce the heat propagation towards the cold mass. For 13.b the heat produced is distributed towards two *ReBCO* tapes on top and bottom of it, isolated electrically by kapton layers. The second tape stack makes better use of the heat produced and ultimately was the configuration chosen as the base design for the switch. Having two *ReBCO* tapes in the stack could mean having two thermally coupled switches, or a single switch if the *ReBCO* tapes are connected in parallel, for a higher electric current. Two examples of connecting this setup are described in the following sections.

3.2.1 Single switch

By connecting the two *ReBCO* tapes in parallel, the current will distribute between them, and overall it will function as a single switch, activated by the heater tape. In Figure 14 the electric current is indicated as a point of an arrow, flowing perpendicularly respect to the plane of the page.

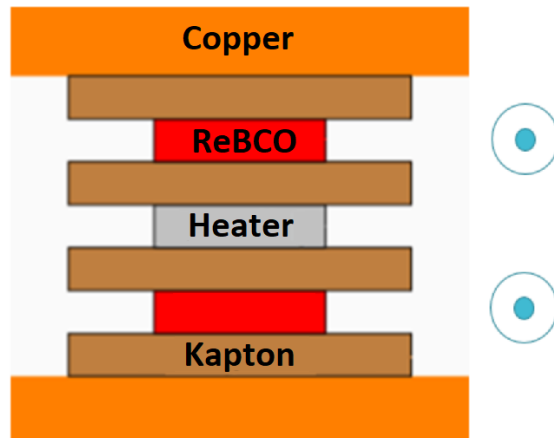


Figure 14: Single switch configuration, the ReBCO tapes are connected in parallel so the electric current (indicated with the arrowhead in blue for each ReBCO tape) flows in one direction.

This configuration then functions as a simple switch that is able to interrupt the current in one conduction line by activating the heater tape.

3.2.2 Double switch

By connecting the two *ReBCO* tapes in series, with a load in between, a double switch is produced, having two thermally coupled switches corresponding to each one of the *ReBCO* tapes, though the total current will be diminished respect with the single switch case. In Figure 15 the electric current correspond to the tip and tail of an arrow, flowing perpendicularly respect to the plane of the page.

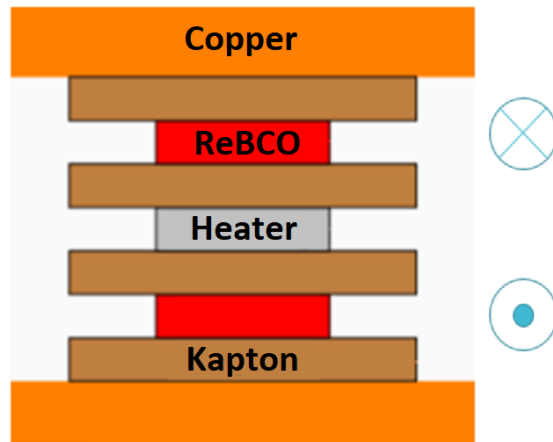


Figure 15: Double switch configuration, the *ReBCO* tapes are connected in series, so the electric current flows in opposite directions, indicated by the arrowhead and arrowtail in blue for each *ReBCO* tape.

This connection scheme is useful for a superconducting rectifier application, since it is needed to activate simultaneously two switches in order to inject current into the respective load. The spatial magnetic field around the tape stack is modified due to the opposite running currents, being the magnitude bigger in the center of the tape stack and comparatively small in its surroundings, which will be shown later.

3.3 Experimental test stand for *ReBCO* switch

As mentioned before, a superconducting switch relies in the change from superconducting to normal conducting state, to then redirect an electric current. Prototypes have been developed by either heating the superconductor or applying an external magnetic field to change its state [17, 18, 49].

A first prototype model of low current superconducting switch has been developed by members of the superconductors research group (EP-ADO) at CERN, shown in Figure 16. *ReBCO* tapes are contained in a copper casing that serves as a heat sink, being partially submerged in liquid nitrogen (77 K), to cool down the whole setup and maintain it below the critical temperature of the *ReBCO* tapes, so they work in superconducting state. Applying an electric current in the heater will make its temperature rise, which in turn will increase the temperature of the *ReBCO* tapes, so they transition towards the normal conducting state (switch "open"). When the current in the heater is turned off, heat will propagate towards the cold mass and the system will reach again the baseline temperature, recovering the superconducting state (switch "closed"). The *ReBCO* tapes and heater are separated by Kapton

foil, to isolate them electrically. The setup has already been tested and measurements have been done with seemingly promising results, which serve as proof of principle to do further research.

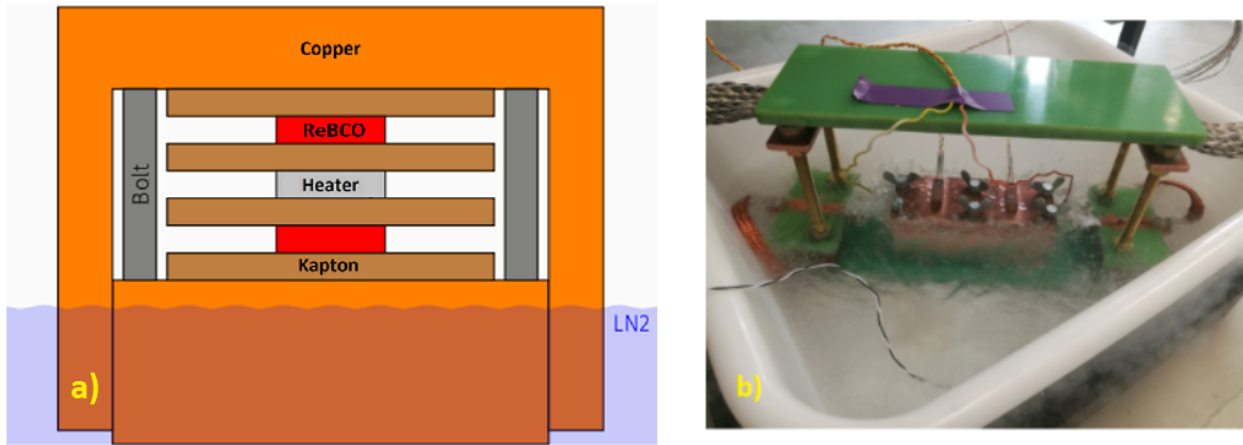


Figure 16: a) Experimental setup of the ReBCO based superconducting switch. Cross section of copper casing (orange) that comprises layers that make the superconducting switch, corresponding to Kapton (brown), ReBCO tape (red) and electric heater (gray). b) Cooling down of the setup is done with liquid nitrogen. From [51].

Figure 17 shows an isometric view of the test stand. The current that flows through the superconducting tapes is injected from one side, as well as the current through the electric heater, but they are independent from each other, coming from different power sources, and separated in the ReBCO switch by the Kapton layers.

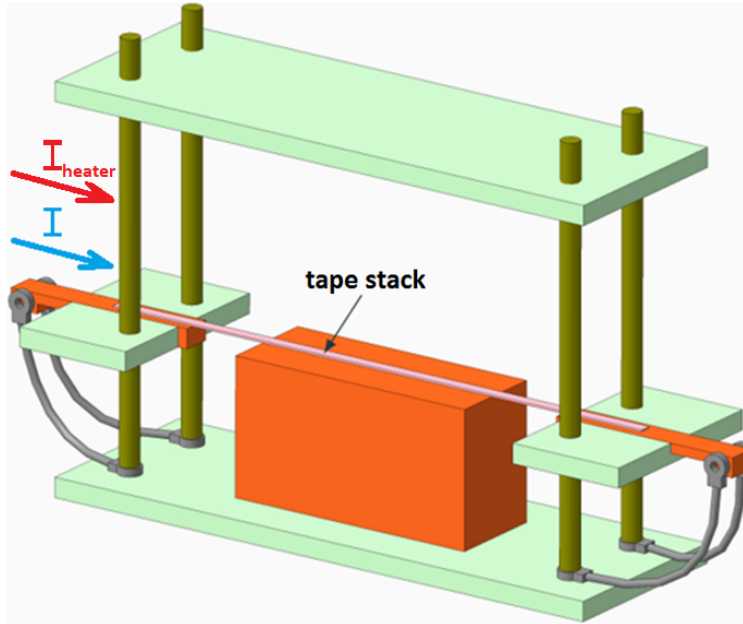


Figure 17: Test stand for the ReBCO switch. The ReBCO tapes are connected in the copper connections on the edges so the electric current flow along. The current I (blue) that runs through the superconductor is independent of the current I_{heater} (red) used to control the open and closed states of the ReBCO switch. From [51].

A next step would be to increase the gate current handled by the device. This can either be done by stacking ReBCO tapes or making use of a high current *ReBCO* cable. Depending on the option chosen, this will require to develop an efficient heating mechanism to change the state from superconductor to normal conductor of the high current cable or stack.

The aim then is to develop, in the framework of this project, a superconducting switch design that can handle 10 kA, to become a first step prototype as relevant technology for superconducting coils. The project comprises the design of the switch, by the means of a simulation model, as well as support to the members of the work group to make the tests in the experimental setup and gathering data, which is then used as a guideline to tune the simulation model.

Regarding the experimental part of the project, mainly developed by the other group members, a gradual increase of the current is done during a number of experiments. A software to control the current injected by the power supply is available in the physical setup, which allowed to set current pulses or currents ramps to test different scenarios, as well as turning off the power supply in case a quench was detected, determined by measuring the voltage across the tape stack, which appears when the total resistance of the tapestack starts growing due to losing the superconducting state.

3.4 Coating of ReBCO tapes

A *ReBCO* tape is conformed of several layers of different materials that overall allow to operate as a superconducting cable with some normal conducting material, usually copper,

which conducts the current in case there is a loss of superconducting state in the tape.

However for the particular application of a superconducting switch, the objective is to have a high resistance when the switch is "opened". This means that the *ReBCO* tape will overall have a lower resistance when a copper layer is present, as can be observed in Figure 8. So then it is expected that the system would work better either by removing completely or leaving a fairly thin layer, which would allow to have an overall resistance as high as possible.

3.4.1 Stabilizer layers in ReBCO switch application

The *ReBCO* tapes available commercially usually include a copper layer as stabilizer. Early tests were done by using them without modifications, however, due to the coating, the resistance achieved while the superconductor switches to normal conducting state was similar to that of the stabilizer. In a switch the open state has a very high resistance, so in order to reproduce this it was deemed necessary to remove the stabilizer coating for this application.

3.4.2 Etching

Etching is called to the process to remove the copper and silver coatings while conserving the superconducting material, in order to increase the resistance of the *ReBCO* tape, and then that of *ReBCO* switch overall.

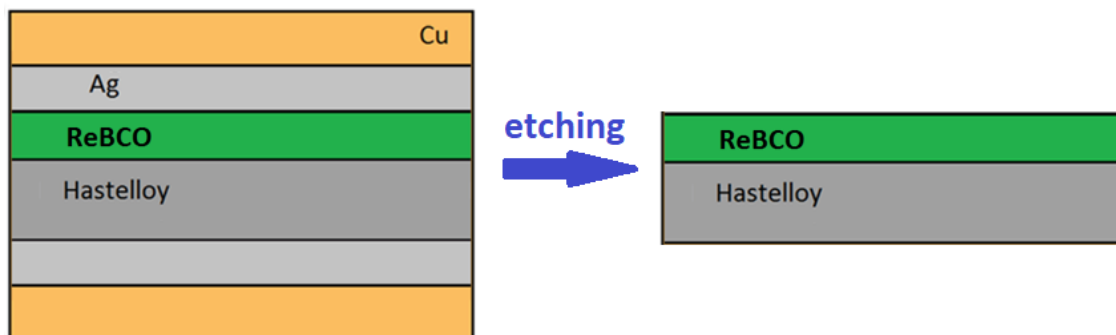


Figure 18: Lateral view schematic of a *ReBCO* tape, subjected to an etching process. Removing the copper and silver stabilizer layers increases considerably its total resistance, feature needed for a superconducting switch application.

ReBCO tapes can be bought with or without the copper stabilizer layer, the latter being usually more expensive since it requires a modification in the manufacture production line. Although it is wanted to remove the stabilizer on most of the length of the *ReBCO* switch, it is still convenient to have copper coating in the edges of the *ReBCO* tapes for making electrical contacts to the power supply.

It was then decided to etch the *ReBCO* tapes on site in order to reduce costs and have the personalized samples used in the experimental setup. There has been some testing into removing the stabilizer while preserving the *ReBCO* material in the tape.

One of these tests has involved the use of ferric chloride ($FeCl_3$), which is a compound

used in electronics to remove copper from printed circuit boards (*PCB*), used in a liquid solution. Then by submerging the tapes, it is to be expected that the outer copper layer from the tape would be removed, and ideally also a thin silver layer that is present as well. However this is not a straightforward process since the timing that the sample gets submerged is crucial to remove the desired layer, with a copper thickness that is not known for certain beforehand, a temperature dependence of the process, and even mechanical agitation that influences the reaction rate. Just by itself, if the sample remains submerged for enough time, both the copper and *ReBCO* material get etched from the tape, leaving behind only the hastelloy layer.

It is still an ongoing process to find the best way to remove the copper layers, which also might require expertise from other research groups.

4 Simulation model of the ReBCO switch

This section explains the thermal and electrical properties that are considered in the simulation model for the *ReBCO* switch. Assumptions and simplifications are applied during the process, with the aim to develop a nonetheless adequate representation of how the experimental setup behaves both in its thermal and electrical behavior.

4.1 One tape stack model

4.1.1 Thermal model 1D

As can be seen, the heat source is in the middle of the tape stack, which can be controlled to change the superconducting state of the *ReBCO* tapes in an operating temperature below the critical temperature of ReBCO material, which is around 92 K, so liquid nitrogen can be used to cool the system. When the heater layer is "turned off", the heat will dissipate towards the copper edges. According to this situation, a simplified one dimensional heat model is established to describe the system according to Equation 2:

$$c(x, T_1)\rho(x)\frac{\partial T_1}{\partial t} = \frac{\partial}{\partial x} \left(k(x, T_1)\frac{\partial T_1}{\partial x} \right) + \dot{q}_{hs1} \quad (2)$$

where for each layer c is the specific heat capacity, ρ is the density, k is the thermal conductivity, \dot{q}_{hs1} is the heat produced by the resistive tape; considering the composition along the vertical direction (x) and temporal evolution (t) of the system, that determine the temperature (T).

As shown in the next section, the *ReBCO* tape are modeled as stacked layers of different materials. Their physical properties, namely the specific heat capacity and thermal conductivity, can be computed in the model as their effective value, related with the volumetric fraction of the each layer respect the total volume of the *ReBCO* tape [57]. Simplifying terms due to the same width and length of the layers result in the following expressions:

$$c_{eff} = \frac{1}{h_{total}} \sum h_{mat}c_{mat}$$
$$k_{eff} = \frac{1}{h_{total}} \sum h_{mat}k_{mat}$$

where h_{total} is the total thickness of the tape, and h_{mat} , c_{mat} , k_{mat} are respectively the fraction thickness, specific heat capacity and thermal conductivity of each material that composes the *ReBCO* tape. c_{eff} and k_{eff} are then used in the thermal model to compute the temperature evolution for the sections corresponding to the *ReBCO* tapes.

4.1.2 Electrical model

The temperature at each position defines the electric behavior, so in the *ReBCO* tape determines its overall resistance, considering that each tape is composed of a superconductor and a stabilizer (normal conductive) part. When the temperature of the tape surpasses the

critical temperature of the superconductor, the *ReBCO* layer becomes resistive and the current flows mainly through the stabilizer part, which is the less resistive path.

The layers in the stabilizer are copper and silver, the *ReBCO* tape contains yttrium as its rare-earth element compound, and the hastelloy is a steel alloy that provides mechanical structure to the *ReBCO* tape. The model, considering this composition, is then defined as shown in Figure 19.

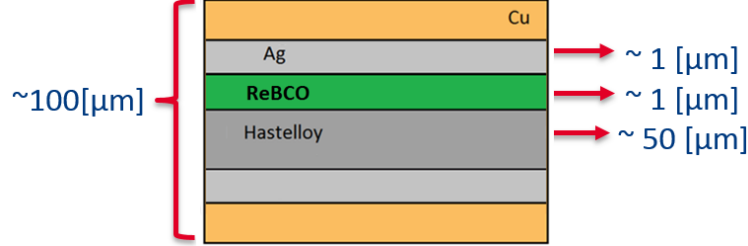


Figure 19: Model in the simulation for the ReBCO tape, showing layers and approximate dimensions, which can be tuned to adjust the model to the experimental data.

The current sharing between superconductor and stabilizer is defined by the electric field across the conducting line. Since the superconducting (SC) and normal conducting (ST) are parallel, the electric field across them is the same, and it is possible to compute the current that flows in each of them in function of their temperature at any given moment, described by the temperature dependent relation so called power law equation (Eq. 1), expressed first as the equal electric fields in function of electric current and temperature and then broken down in each of their specific terms:

$$E_{sc}(I, T) = E_{st}(T)$$

$$E_0 \left(\frac{J_{sc}}{J_c} \right)^n = \eta_{st} \frac{I_{st}}{A_{st}} \quad (3)$$

The terms on the left correspond to the already introduced power law. The terms on the right correspond to the electric field in the stabilizer part, where η_{st} is the overall resistivity of the stabilizer materials, I_{st} is the current running through the normal conductive part and A_{st} is the cross sectional area.

The overall resistivity for the model, considering that is composed of layers of different materials, is dependent of the resistivity of each material and the volume fraction from the total that each material occupies. Considering that all layers have the same width and length, this is dependent only of the relative thickness respect the total, and then has the form of:

$$\eta_{st} = \frac{h_{total}}{\sum \frac{h_{mat}}{\rho_{mat}}}$$

where h_{total} is the thickness of the *ReBCO* tape, h_{mat} and ρ_{mat} are the thickness and resistivity respectively for each material.

The total current that flows in an *ReBCO* tape at any time is the sum of the current in SC and ST, and the distribution of it will change in function of the temperature, as exemplified in Figure 20.

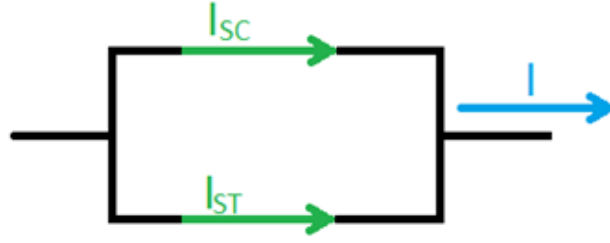


Figure 20: Current sharing between superconducting and normal conducting layers. I is the total current that flows through the ReBCO tape.

From the electric currents running through the superconducting and stabilizer parts, consider that an electric field is produced when the resistivity of a tape starts rising due to surpassing any of their critical parameters. A joule effect is produced from this overall resistance and the total current running through the device, which can be separated in its superconducting and stabilizer parts, or computed as the total power produced:

$$q = q_{sc} + q_{st} = EI_{sc} + EI_{st}$$

$$q = EI \quad (4)$$

where q is the total power loss, E is the electric field produced across the conducting line, I is the total current. q_{sc} , I_{sc} and q_{st} , I_{st} are respectively the power loss and electric current contributions for superconducting and stabilizer parts.

Finally, the performance of the *ReBCO* switch is described by the time it takes to change its superconducting state. These four terms are further on referred as the ***time response*** for the system:

- *Rise time delay* (τ_{delayR})
Time delay from when the heat pulse is applied until the ReBCO material gets heated enough to start changing to normal conducting state;
- *Fall time delay* (τ_{delayF})
Time delay from when the heat pulse stops until the ReBCO material gets cooled down enough so it begins to become superconducting again;
- *Rising time* (τ_{rise})
Time to change from superconducting to normal conducting state;
- *Falling time* (τ_{fall})
Time to restore superconducting state, when tape is cooled down.

The time response parameters are shown graphically in Figure 21.

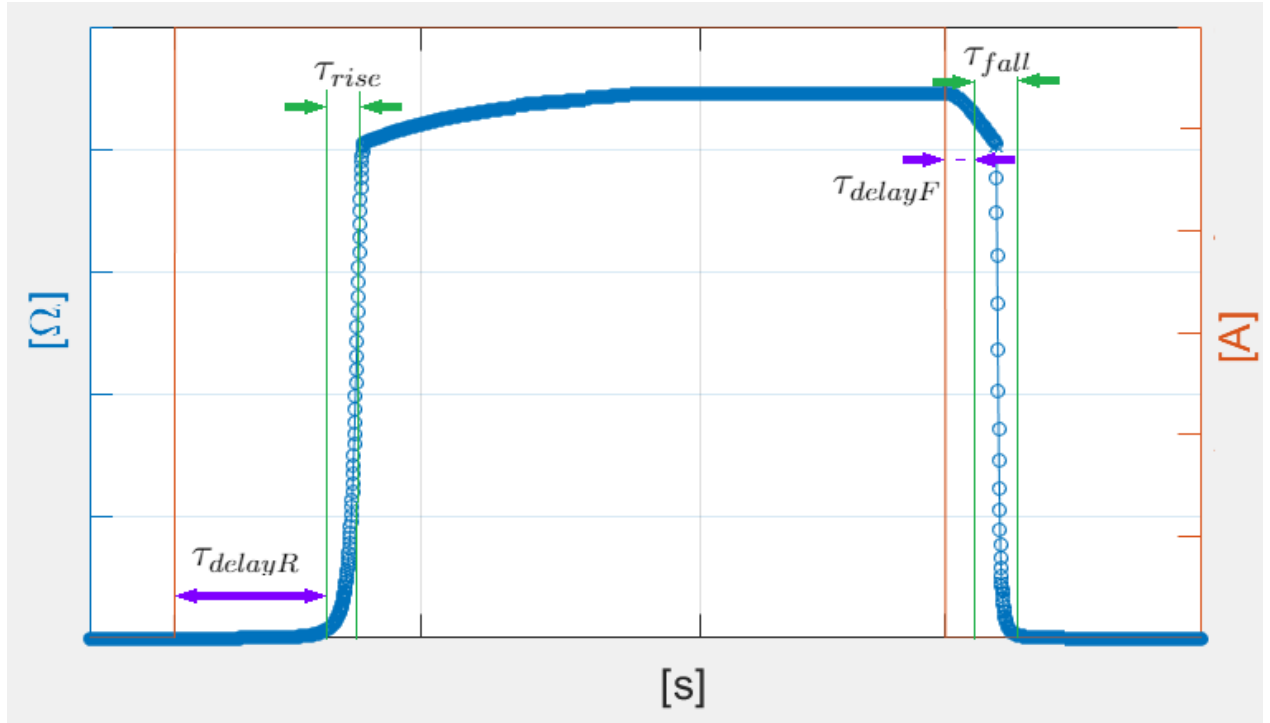


Figure 21: Schematic for a Resistance vs Time plot, showing the time response parameters. A heat pulse is applied with a step current (orange), and there is an increase in the resistance due to surpassing the critical temperature (blue). The delay times are shown in purple, rising and falling times appear in green.

And then, the maximum switching frequency, in this case how fast the switch can be turned on and off in a cyclic manner, corresponds to the inverse of the sum of the 4 terms previously mentioned:

$$f_{switch} = \frac{1}{\tau_{switch}} = \frac{1}{\tau_{delayR} + \tau_{delayF} + \tau_{rise} + \tau_{fall}} \quad (5)$$

4.2 Two conducting lines model

The switching behavior between the current that flows in 2 separate superconducting lines is produced. The reason being to understand how the current will flow towards the second branch when the first one is switched (heated so it becomes resistive). This in turn will allow to compute the response time and the current sharing behavior in both lines as function of temperature. The cross section of such configuration is shown in Figure 22.

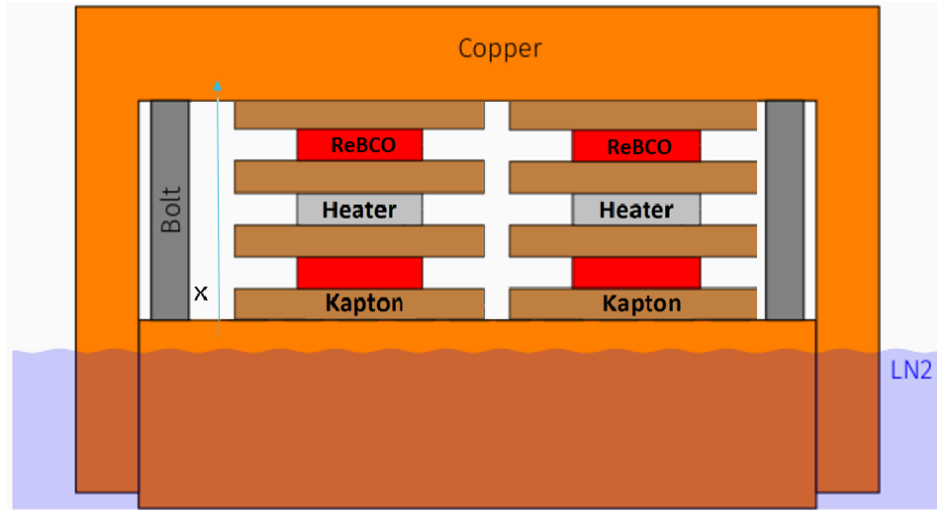


Figure 22: Simulation scenario for the current sharing between two superconducting lines, both of them in the single switch case. When one of them is quenched the current is redirected towards the other branch.

As in the case for a single tape stack, there will be a distribution of current between superconductor and stabilizer for each tape, schematically shown in Figure 23.

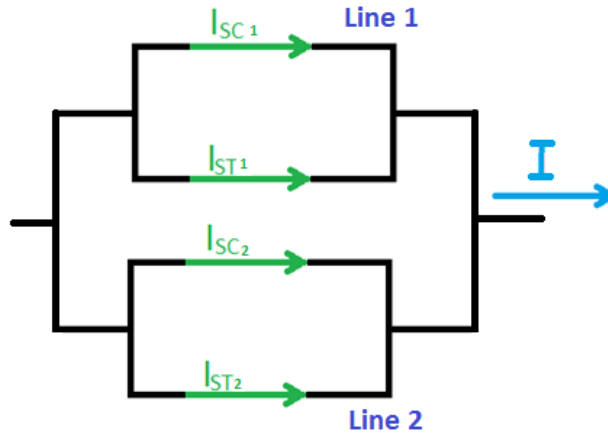


Figure 23: Current sharing between superconducting and normal conducting layers for two conducting lines. Each conducting line has its respective ReBCO tapes, hence its own superconducting and resistive material layers.

Since both tape stacks are connected in parallel, they behave as two resistors, so the voltage in the two end points is the same at any given moment. And the total current in the two tapes is always conserved. This describe five equations that hold for the system, 3 of them in the form of the electric field for superconductor and stabilizer for both tapes and another one for current conservation, that additionally with the corresponding 1D heat model for each tape form the system of equations (6):

$$c(x, T_1)\rho(x)\frac{\partial T_1}{\partial t} = \frac{\partial}{\partial x} \left(k(x, T_1)\frac{\partial T_1}{\partial x} \right) + \dot{q}_{hs1} \quad (6a)$$

$$c(x, T_2)\rho(x)\frac{\partial T_2}{\partial t} = \frac{\partial}{\partial x} \left(k(x, T_2)\frac{\partial T_2}{\partial x} \right) + \dot{q}_{hs2} \quad (6b)$$

$$E_{sc1}(I_1, T_1) = E_{st1}(T_1) \quad (6c)$$

$$E_{sc2}(I_2, T_2) = E_{st2}(T_2) \quad (6d)$$

$$E_{st1}(T_1) = E_{st2}(T_2) \quad (6e)$$

$$I_0 = I_{sc1} + I_{st1} + I_{sc2} + I_{st2} \quad (6f)$$

By solving the system of equations it can be determined how an electric current switches from one conducting line to the other, by heating one of the tape stack so it will cut the current running through it while the other branch takes the full current running in the tape stack.

Then, having two conducting lines system as in Figure 22, this means that the total current will distribute between superconductor and stabilizer of each tape, and of each conducting line in function of the temperature mainly (magnetic field also has an effect, but this is negligible for small currents up to a few hundred amperes).

Consider then that the tapes are connected as shown in Figure 23. If the tapes are the same there will be an equal sharing of the total electric current flowing through them, so by turning on the heater in one of them there will be a resistance due to the change to normal conducting state, so the total current will flow through the other conducting line that is superconducting. Then the heat pulse is stopped and the system is cooled down again, the heated branch becomes superconducting again and both of them then conduct equally the total current. Then the second heater is activated, the branch becomes normal conducting and the total current flows through the superconducting branch, and the situation is repeated.

4.3 Considerations for a high electric current ReBCO switch

Going to higher electric currents can be done by stacking *ReBCO* tapes, so in joint effort they will be able to conduct a higher value. However this produces additional effects that need to be taken into account, such as an overall slower heat propagation due to the increased thermal resistance from multiple *ReBCO* tapes, and the self generated magnetic field.

4.3.1 Vertical tape stacking

Although the *ReBCO* tapes by themselves are fairly thin, about 100 [μm], stacking them will reduce the rate at which the system is both heated up and cooled down. For this reason it's possible to test different tape stack configurations to determine the best one for this time responses by switching the superconducting state of the tape stack. The procedure to increase the number of *ReBCO* tapes is shown in Figure 24, adding parallel layers on top and bottom to increase the total current that can be conducted by the stack.

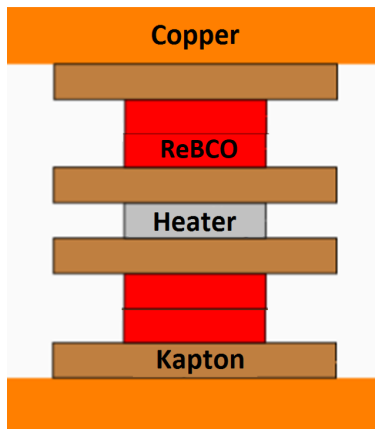


Figure 24: High current thermally activated ReBCO switch with 4 tapes. For a single switch configuration all the ReBCO tapes are connected in parallel, to increase the total current that can be conducted. For a double switch configuration, the ReBCO tapes for the bottom part are connected in parallel, as well as the ones for the top; and in the end, these top and bottom sections are connected in series.

4.3.2 Interlayer thermal contact

An additional consideration is that there could be a non-uniform thermal contact between stacked *ReBCO* tapes, due to defects in the materials or small gaps, which also leads to a delay in the heat propagation. A simplified way to estimate this effect is to model between tapes a very thin layer of an isolating material (Kapton in this case), so as to allow some tuning of the model while comparing with experimental data once a particular configuration is chosen.

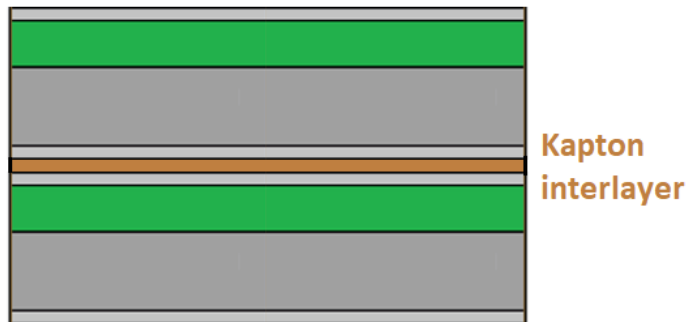


Figure 25: Schematic for a thermal contact interlayer between two etched ReBCO tapes (note that there is still a thin silver layer remaining). The thin kapton layer serves as tuning value for the heat propagation between the ReBCO tapes for a non-uniform contact between them.

In Figure 26 it is shown a temperature profile along the vertical direction of the tape stack for 3 tape pairs given a heat pulse, where it can be observed small temperature drops in between the *ReBCO* tapes due to a non-uniform thermal contact.

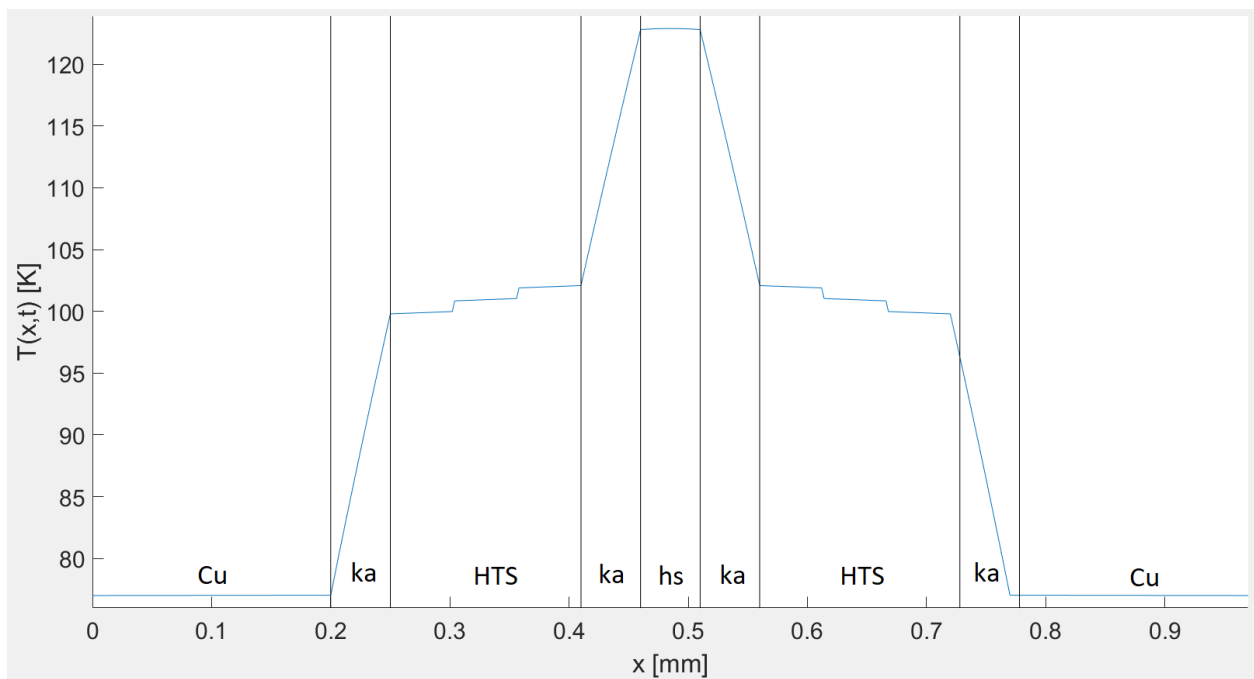


Figure 26: Temperature profile vs Vertical length, showing the effect of non-uniform thermal contact on temperature distribution for a 6 ReBCO tapes stack when a heat pulse is applied. The horizontal axis correspond to the length along the vertical axis in the tapestack, and the black vertical lines divide between the different material layers present in the tapestack. Note the drop in temperature between each ReBCO tape.

4.3.3 2D Magnetic field

An electric current produces a magnetic field in its surroundings. For low currents in a flat conducting tape, the magnitude of the self field is relatively low so it's effect is negligible. However for currents in the kA range the magnitude of this self field is already considerable (in the hundreds of mT). So this effect causes that the operational margin in the superconducting state to become narrower, since the operational point goes closer towards the critical surface of the superconductor. So, when operating at a high electric current, the current density in a superconductor gets diminished due to the self magnetic field, along with any present external magnetic field, which further enhances the effect.

For the case of interest of this project, a set operating temperature for the tapestack is defined, below the critical temperature of the superconductor. Then, the critical current of the device (i.e. the maximum current that can be conducted through the device) is dependent on the critical current density at the set operating temperature, considering the magnetic field that is produced with this maximum current.

In Figure 27 it is shown a cross section of a tape stack with size $(2w \times 2b)$. The current flows along the z axis. Assuming an infinite line conductor with cross section $d\xi \times d\eta$ at point (ξ, η) , carrying a current density j , produces the magnetic field strength h_p at point $P(x,y)$.

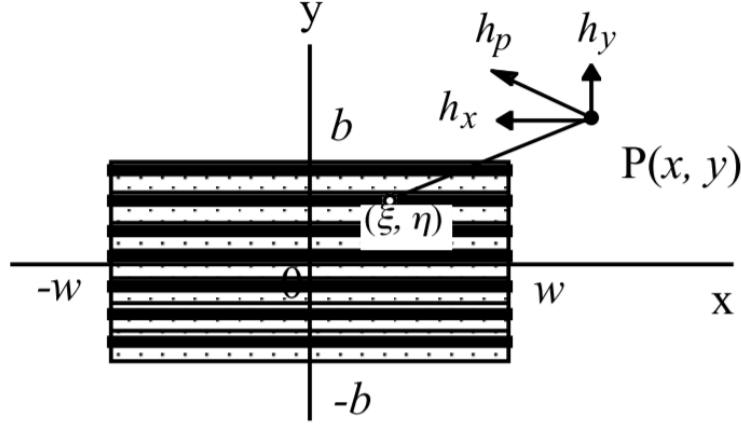


Figure 27: 2D magnetic field strength in a point P generated by stacked ReBCO tapes. Each tape carries an electric current, that in joint effort create a self magnetic field, which diminishes the attainable critical current. From [32].

From Biot-Savart law, the magnetic field strength components h_x and h_y , of h_p , can be obtained, which in turn define the 2D magnetic field B :

$$\begin{aligned}
 h_x &= -\frac{j(y-\eta)}{2\pi[(x-\xi)^2+(y-\eta)^2]}d\xi d\eta \\
 h_y &= \frac{j(x-\xi)}{2\pi[(x-\xi)^2+(y-\eta)^2]}d\xi d\eta \\
 B &= \mu_r H
 \end{aligned} \tag{7}$$

The field components are integrated along the conductor for each tape where the current locally flows (for the simulation mode, a numeric integration by a discretization of the 2D space). This in turn allow to determine the total magnetic field in the 2D space produced by the square *ReBCO* tapes (in cross section) of the tapestack, which defines a total critical current, which is lower than what the total critical current would be if no magnetic field was considered [32, 58].

Then, by integrating along the 2D space the critical current density, the total critical current for a tapestack of n *ReBCO* tapes is obtained:

$$I_c = \int \int j_c(B_c(h_x, h_y), T_0) dx dy \tag{8}$$

where the magnetic field B_c is a function of the magnetic field strength components h_x and h_y , set at the operating temperature T_0 .

Since the electric current and magnetic field are interrelated, first a critical current distribution along the tapes is defined as an initial guess, for which the magnetic field is computed and then the corresponding critical current density. This process is iterated in order to determine the resulting magnetic field and its corresponding critical current distribution along the *ReBCO* tapes.

5 Results

In this sections the results from the simulation model are presented. The equations described in the previous sections are solved numerically in the MATLAB environment, so the data output is then treated to present the parameters for the thermal and electrical response of the system, the current sharing between two conducting lines when one of them is quenched by a *ReBCO* tapes, and finally the magnetic field produced for a high current tape stack.

The measurements obtained by making tests with the experimental setup serve as a validation and tune up guide for the simulation model. The time response (which depends on how the heat propagates through the tape stack) and resistivity increase when surpassing the critical current, are presented.

5.1 Model tuning process

As seen in Figure 8, a *ReBCO* tape is conformed by layers of different materials. A simplified model was developed with the materials that make most of the *ReBCO* tape composition, that then have a bigger impact in its behavior. Additionally, while computing the heat propagation through the different layers, average values are used for the cases of the specific heat capacity and thermal conductivity, which then function as a single material to solve the heat equation.

Furthermore, the thickness of the different layers define the overall resistance of the *ReBCO* tape, so these dimensions can be modified within the range of the total thickness of the tape. This process allows to compensate the unknown factors and then get a model which resembles the behavior of the real system, comparing measurements and simulating them under the same conditions.

5.2 Simulation Output

5.2.1 Thermal response

By solving Equation 2 the temperature over time along the defined space vector is defined, by plotting these 3 variables, then Figure 28 shows the resulting temperature surface in function of distance and time:

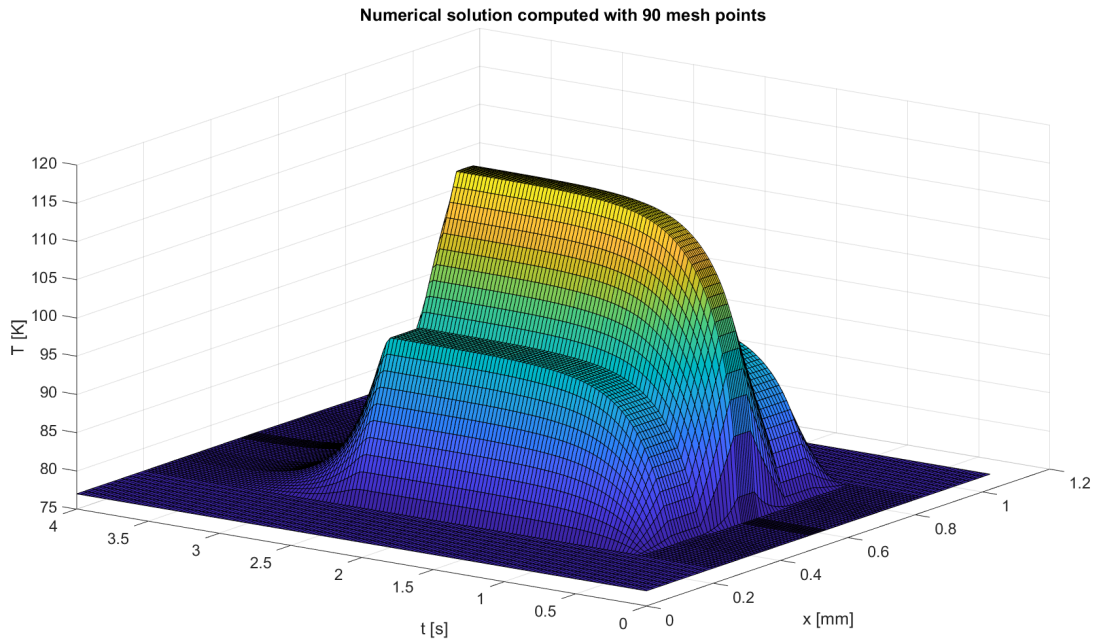


Figure 28: Temperature evolution, in function of time and the vertical dimension. Simulation run for a 2 ReBCO tape setup at 77 K, where a heat pulse is applied for 2 [s]. The dimension and time axis are on the horizontal plane, whereas the temperature is on the vertical axis.

Figure 29 shows the the temperature evolution over time due to a heating pulse, calculated in two points in the tape stack, at the center of the heater layer and at the center of the bottom *ReBCO* tape. Also is shown temperature profile along the vertical direction, where the black vertical lines indicate the regions when there is a change from material from one layer to the next:

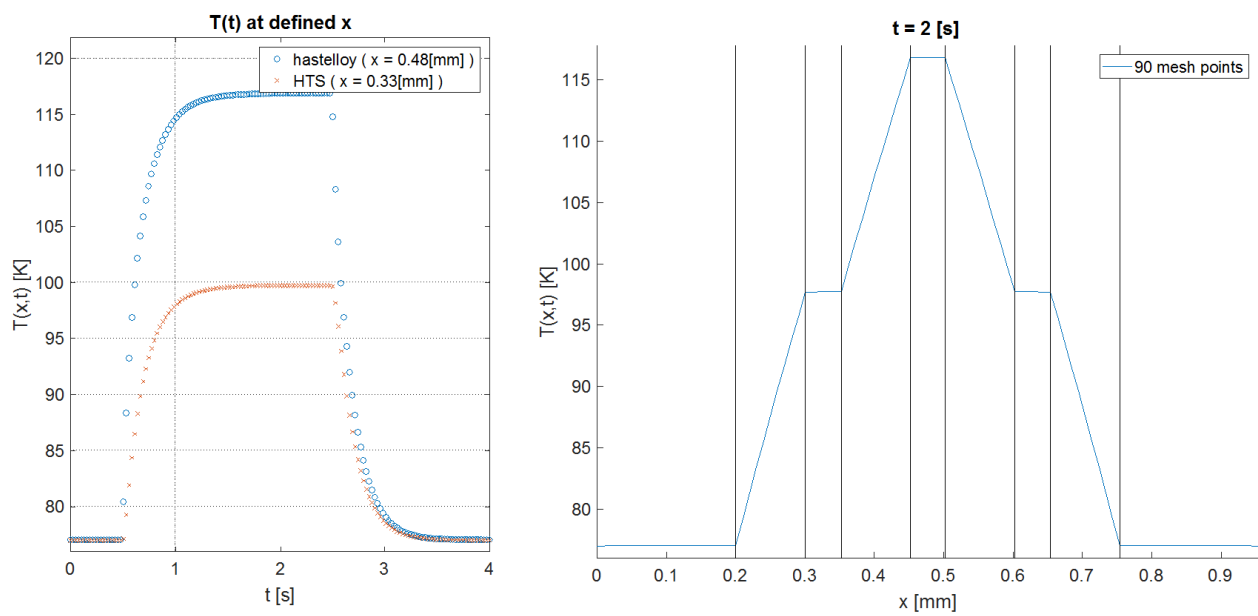


Figure 29: Temperature evolution over time (left) and temperature profile at a given time (right) for 2 ReBCO tapes setup. These correspond to cuts in the temperature surface shown in the previous figure.

5.2.2 Resistance over length

For the high current scenario, the fact of having multiple stacked *ReBCO* tapes means that the thermal resistance will keep increasing as more layers are added in the tape stack, also having more tapes means having more parallel resistances when the switch is opened, decreasing the overall resistance of the switch. In Figure 30 it can be seen this effect, in a single switch configuration, by applying a step heat pulse, the switch gets opened, and after the pulse finishes it gets cooled down again by the cold mass. As can be seen, increasing the number of tape pairs, while increasing the total current that the tape stack can handle, it also leads to a lower overall resistance and a slower cool down time.

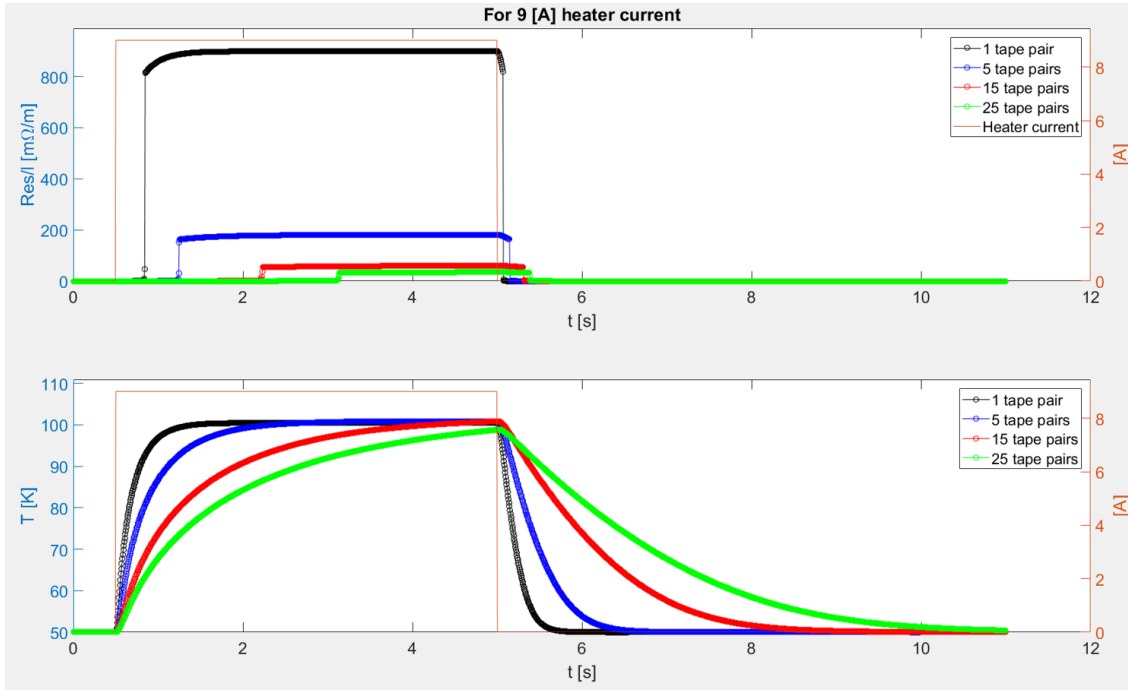


Figure 30: Overall resistance and time response, with 4 different curves for increasing number of *ReBCO* tapes connected in parallel. The top plot correspond to the decreased overall resistance when using more tapes, while in the bottom plot there is a slower switching time because of increasing the thermal resistance towards both the heat source and heat sink.

5.2.3 Time response

In Figure 31 it is shown the four time response parameters of the system when a heat pulsed is applied and the switched is "activated".

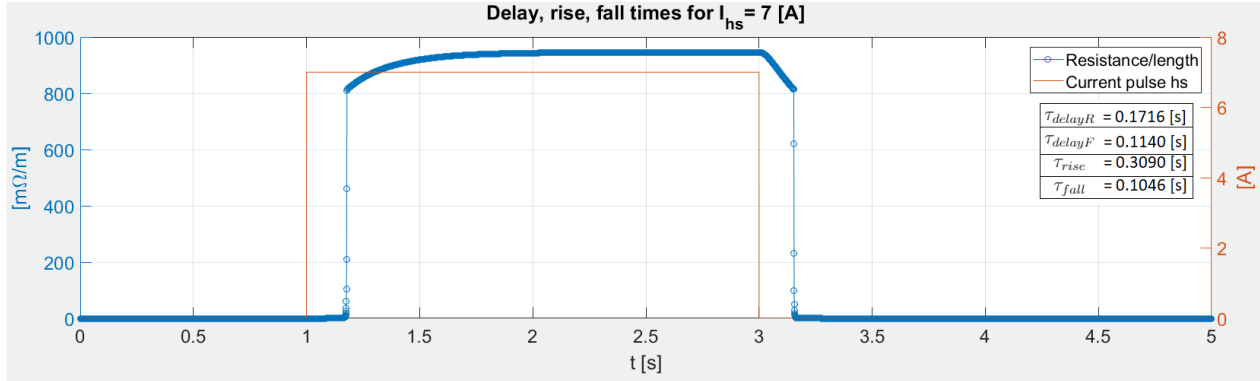


Figure 31: Time response for a heating pulse, for 2 etched ReBCO tapes in single switch configuration. The change of superconducting state can be observed as a rise in the resistance across the ReBCO tapes.

The vertical axis on the left show the resistance per unit of length of the conducting line, and on the right is the magnitude of the electric current applied to the heater. The time is on the horizontal axis. There is some delay between the start of the heating pulse and the change of the superconducting state, due to the time that it takes for the *ReBCO* tapes to increase the temperature and surpass the critical temperature of the *ReBCO* material, as well as the delay from when the heat pulse is stopped and the material is cooled down by the surroundings. The change from superconducting to normal conducting state and viceversa are considerably faster as expected from the sharp transition of these phenomena when any of the critical values is surpassed.

5.2.4 Current sharing between two conducting lines and power losses

Figure 32 shows how the current flows from one branch to the other, for the two conducting lines case. The left vertical axis correspond to the total electric current that flows through all the superconducting elements in the system, the right axis corresponds to the amplitude of the current used to activate the heaters for each branch, having a delay between them to allow that the system gets restored to the superconducting state, so when one branch is heated the other one carries the full electric current.

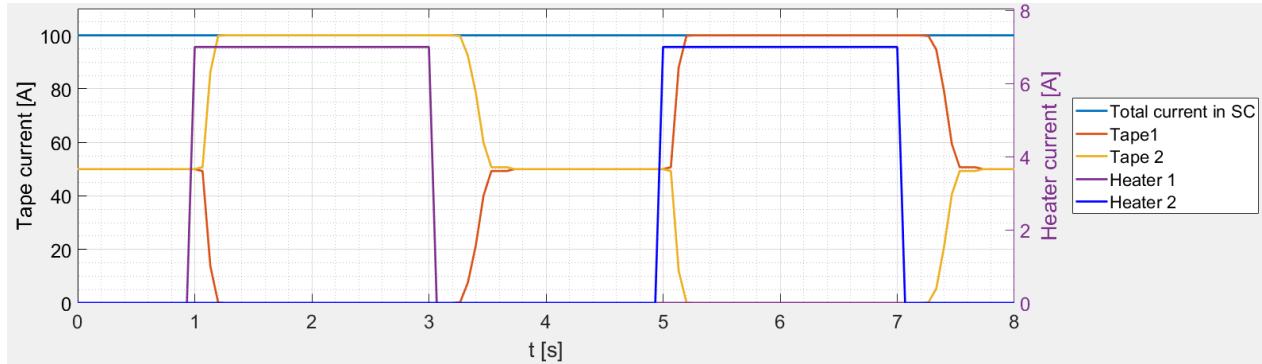


Figure 32: Current distribution vs Time, between conducting lines for two separate heat pulses in each conducting line. Observe that the electric current runs towards the opposite branch when its heater is activated.

As a testing scenario, in Figure 33 it was considered two conducting lines where the respective *ReBCO* tapes have different thickness of the *ReBCO* layer, so the total current in the system would distribute accordingly between these two different cases, however only one line is able to handle the total current, while for the other the critical current would be surpassed.

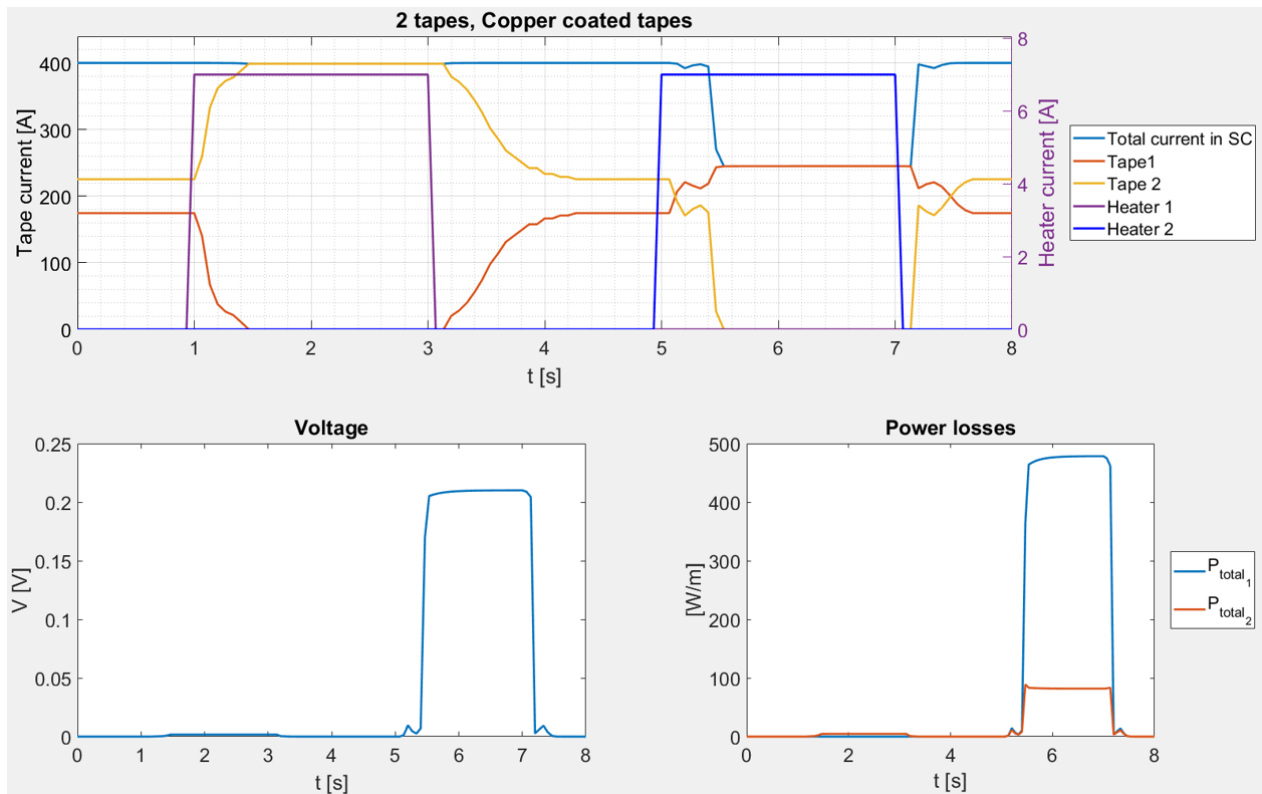


Figure 33: Current distribution vs Time, between non-equal lines when activating each ReBCO switch separately. Voltage across the line (induced resistance times current) and Power losses produced vs Time, in lower plots. Note the effect in the second conducting line, produced by surpassing the critical current density.

Then there are two results. For one the total current gets distributed non-equally, due to one of the branches having a higher cross sectional area for current to flow. When the first heater is activated the current gets conducted in the cold line, however, when the system is cooled down again and the second heater is activated, the line is not able to conduct the total current, only the current below the critical current of the line, while the rest of it flows in the stabilizer sections, inducing a voltage and producing power losses. It is this voltage the one that is used for detecting a loss of superconductivity in a system.

5.2.5 Magnetic field

From the model it is possible to compute the magnetic field in the 2D cross section of the tapestack, considering a set number of *ReBCO* tapes. An overall magnetic field in the 2D space is generated by all the *ReBCO* tapes, and by taking the magnitude of the total magnetic field at each point along the horizontal dimension in each *ReBCO* tape, the local current density can be determined. Repeating the process then defines the current density distribution for all the *ReBCO* tapes in the stack.

In Figure 34 it can be observed the calculated magnetic field distribution in two dimensions for a 4 tape pair stack configuration (8 tapes in total), where the *ReBCO* tapes are shown in bold black rectangles. The red arrows show the local direction of the magnetic field and the colored contour lines represent the magnitude at each point in space. It is considered that the system is operating at a temperature of 50 K, and each tape carries an electric current in an outward perpendicular direction respect to the plane of the page.

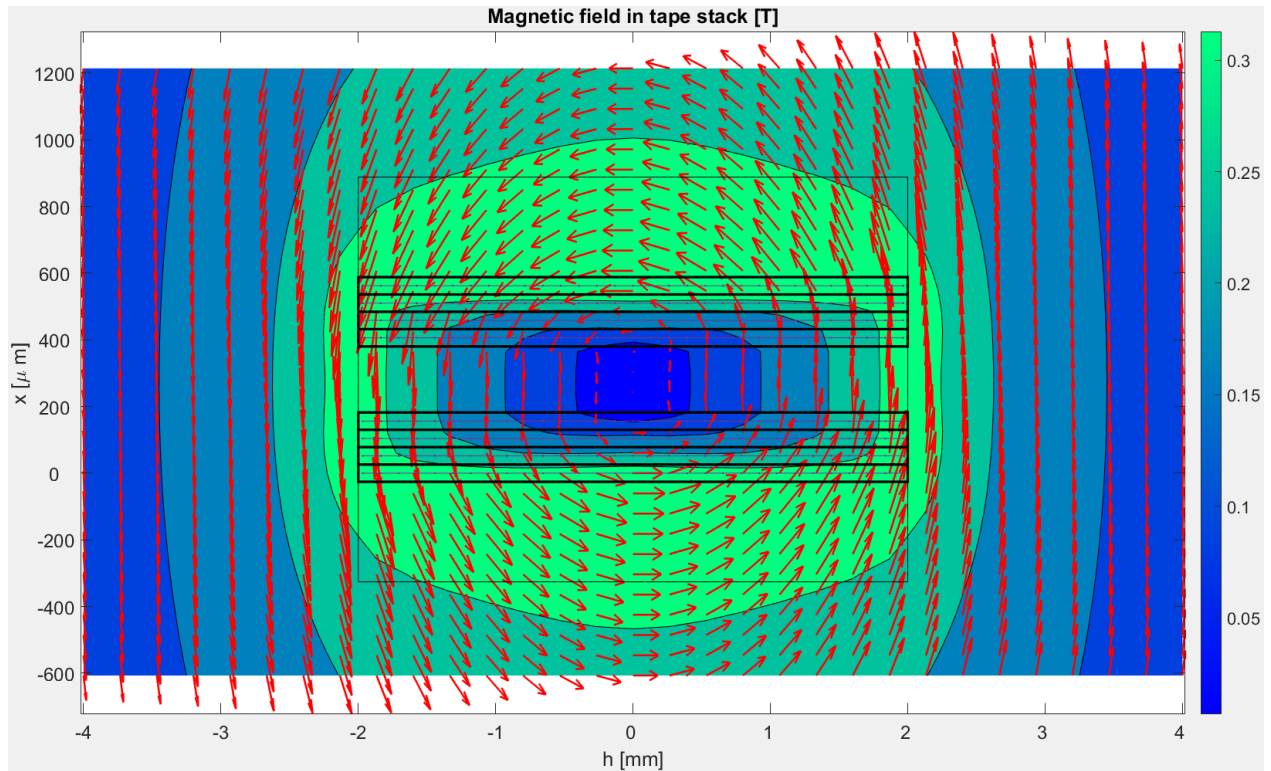


Figure 34: 2D magnetic field calculated for 4 tape pairs, single switch configuration at 50 K. The red lines indicate the direction of the magnetic field and the contour surfaces represent the total magnitude of the magnetic field along the 2D space.

For the same tape stack configuration, in Figure 35 is shown the magnetic field magnitude and critical current distribution along the horizontal direction of the first 4 tapes from bottom to top. There is symmetry respect an horizontal line that passes through the center of the tape, so the variables for the upper tapes are mirrored respect to the bottom ones.

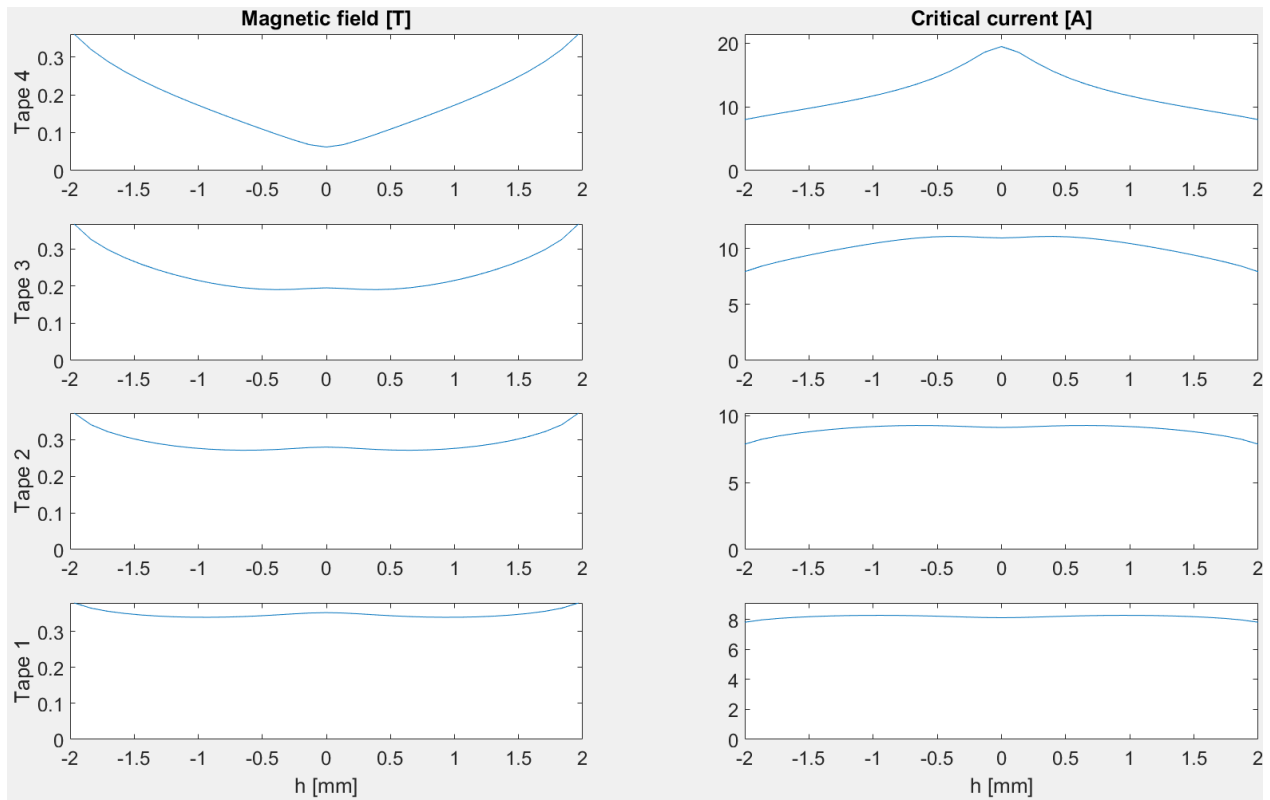


Figure 35: Magnetic field magnitude and Critical current distribution vs Horizontal length, for 4 tape pairs. Single switch configuration at 50 K, showing the first 4 ReBCO tapes from bottom to top, since the values are symmetric respect the heater tape to the last 4 top ReBCO tapes.

As can be observed, there is a non-uniform magnetic field distribution in a cross sectional plane of the tape stack, this means that although the system can be operating at the same temperature, the self induced magnetic field will cause a non-uniform current distribution in each tape.

By connecting the tape stack in a double switch configuration the spatial distribution of the magnetic field changes respect with the single switch. The magnitude is high in the center of the tape stack and low in its surroundings, which also results in a slightly higher total critical current. Figure 36 shows the 2D magnetic field spatial distribution:

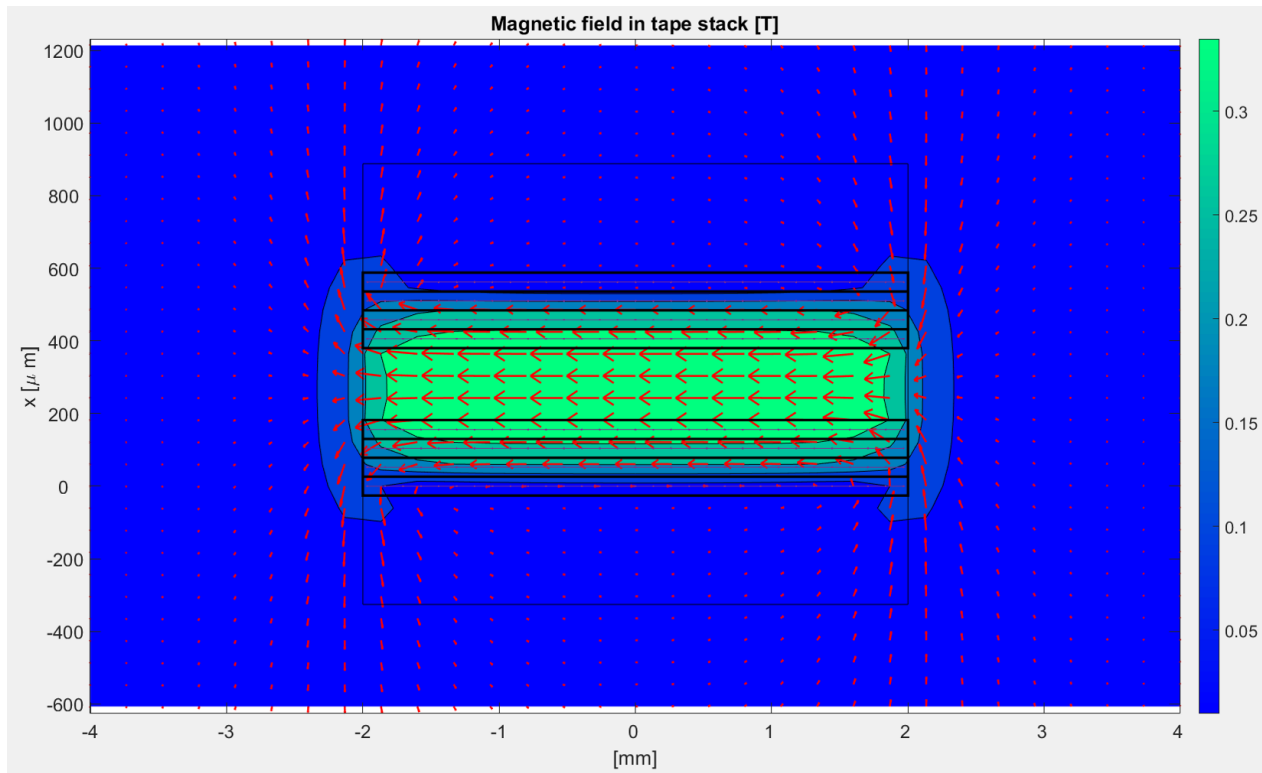


Figure 36: 2D magnetic field calculated for 4 tape pairs, double switch configuration at 50 K. The opposite direction of the current in the bottom and top sections change the distribution of the magnetic field, making its magnitude higher in the center of the tapestack and lower in its surroundings.

5.3 Measurements in test stand

The measurements are done by submerging the system in liquid nitrogen, hence the operating temperature is close to that of the boiling point of nitrogen, 77 K.

5.3.1 Resistance per unit length

In Figure 37 there is a comparison between measured experimental data and the model. It is a single switch configuration carrying a current of 5 A in superconducting state and then, by activating the heater and increasing gradually the power, the temperature in the tape stack starts rising and when the critical temperature is reached there is a transition to the non-superconducting state at around 25 W, and a gradual resistance increase as the heating power increases, which corresponds to the resistance of the stabilizer materials.

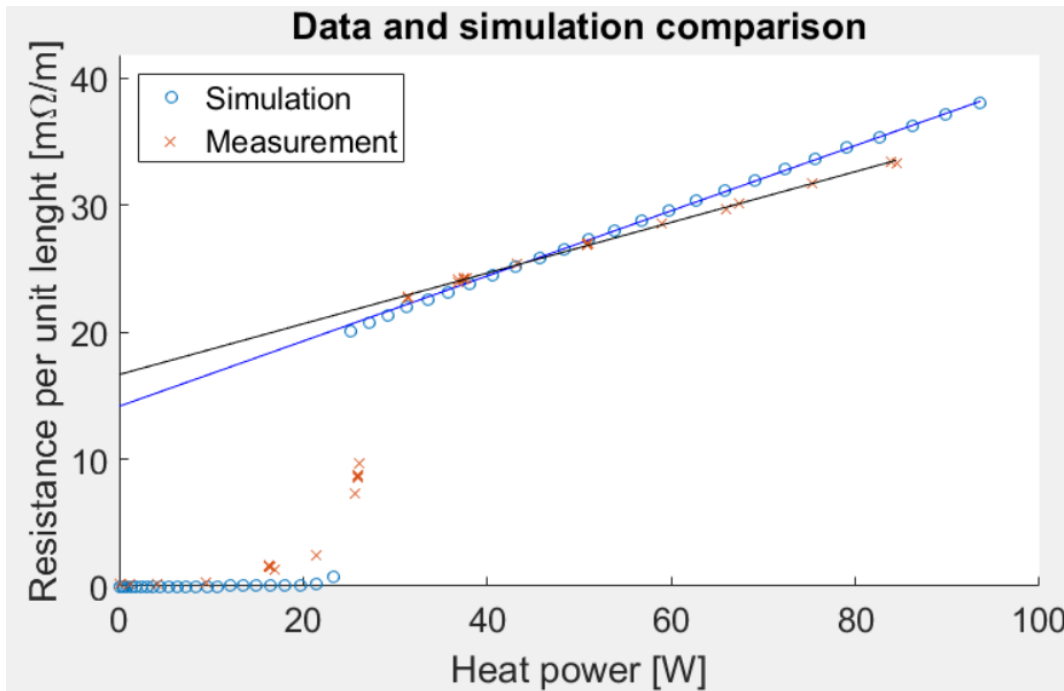


Figure 37: Resistance per unit length vs Heating power. Comparison between simulation and experimental data for a non-etched tape. A linear fit for the non-superconducting regions of the data is shown with straight lines (which correspond to the linear resistivity increase of the regular conducting materials in function of the temperature), along with the respective equation.

5.3.2 Time response

The following measurements were done for non-etched tapes in a single switch configuration. In Figure 38 the top plot corresponds to the simulation, whereas the bottom plot is experimental data for a heater current pulse of 6 A, with the focus on comparing the time response. The resistance over length and voltage for simulation and experimental data respectively are plotted, to compare the shape of the transition between superconducting and normal conducting cases, observing that there is a close agreement between them, as well as with the time response values.

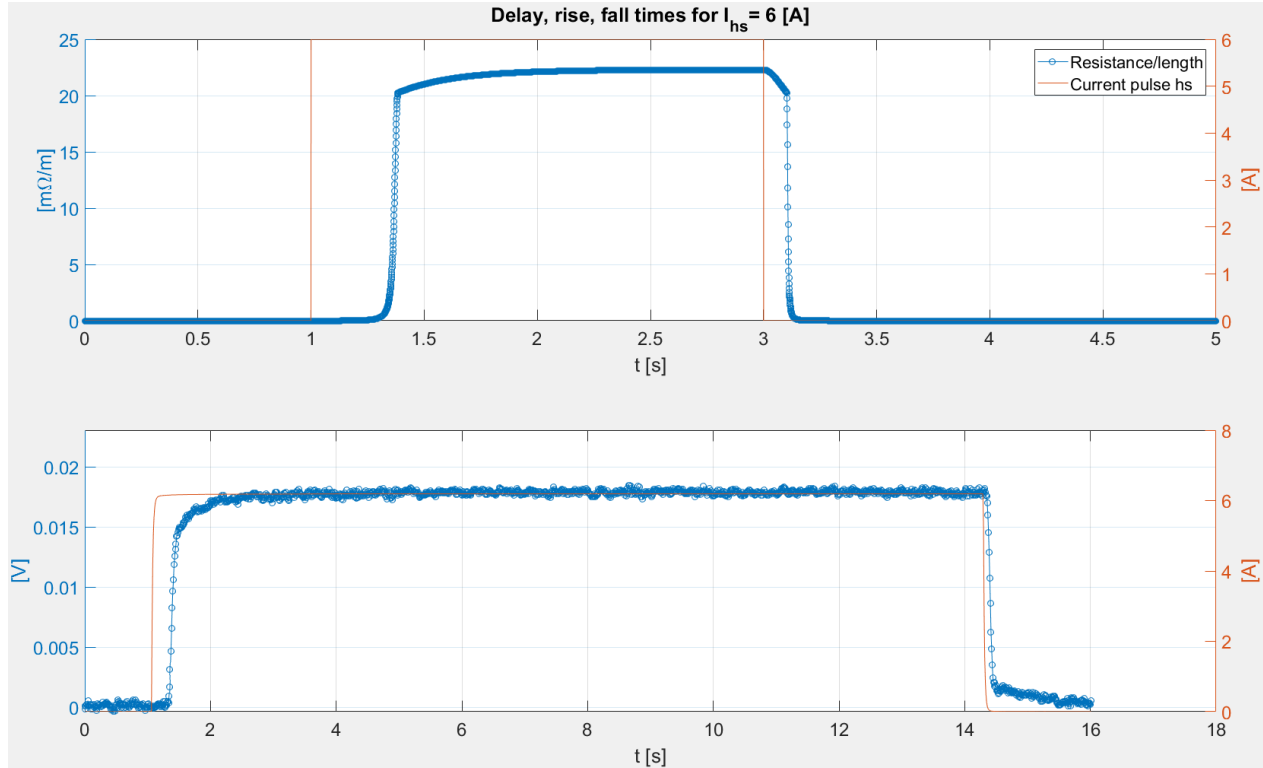


Figure 38: Top: Resistance per unit length vs Time. Bottom: Voltage vs Time. A time response comparison for 2 non-etched ReBCO tapes, at 77 K. There is a heat pulse produced by a 6 A current, and then the increase and decrease in temperature opens and closes the ReBCO switch.

Table 2 shows the comparison for the time responses between the simulation and experimental data, where it can be observed that there is a reasonable agreement between them:

	Simulation	Experiment
τ_{delayR} [s]	0.2951	0.2901
τ_{delayF} [s]	0.1268	0.1201
τ_{rise} [s]	0.1183	0.1143
τ_{fall} [s]	0.0349	0.4156

Table 2: Time response comparison between simulation and experimental data.

Note that there is a discrepancy for the τ_{fall} parameter for the experimental case. Although there is a sharp restoring again towards the non-resistive state, this is not completely zero after the sharp fall, but it is extended a couple hundred of milliseconds, this situation is addressed in the "Discussion" section.

On the other hand, for the simulation case the data is in resistance units, whereas in the experimental data is in volts. This can be converted considering the total current that is running in the superconducting and the length of the ReBCO tape, making use of Ohm's law. Since the previous values are constant, this shifts the data in the vertical direction only, and the proportionality in the horizontal time axis is conserved, reason for which the data parameters can be compared.

For Figure 39 the same situation for the previous case is computed, but ranging across different currents and plotting directly the time responses. For lower values, between 5 and 6 A, the agreement is slightly off due that the temperature of the tape stack is below the critical temperature for the transition to normal conducting state. From 6 A and on, the simulation has a better agreement and follows more closely the trend of the experimental data. Since only four experimental data points were available from the measurements the obtained experimental curve is not smooth.

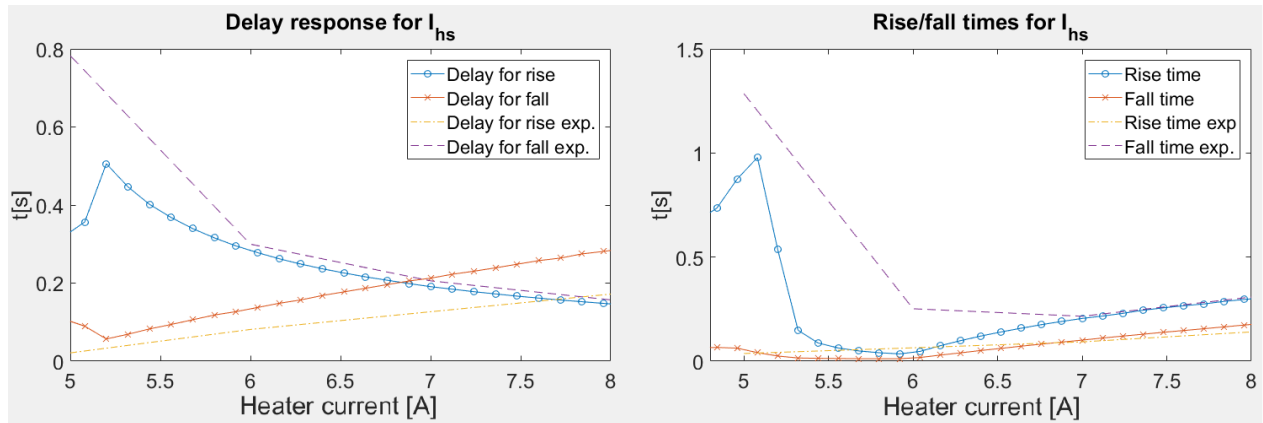


Figure 39: Time response values vs Heater current both for simulation and experimental data. A comparison for non-etched tapes. Multiple heater electric currents where it can be roughly observed the same behavior for increasing heater currents.

6 High current ReBCO switch proposal

6.1 Superconducting rectifier as goal for design

With the intention to develop the *ReBCO* switch in the framework of a project in applied superconductivity, it was designed with the purpose to be part of a *ReBCO* based superconducting rectifier currently in development by members of the EP-ADO group at CERN.

As shown in Figure 11, the device is conformed from 3 basic elements: a transformer to transmit an AC current from an external power supply, a rectifier to convert said current to DC current, and an inductive load to be charged, in this case a superconducting coil made with *CORC* cable. The load is intended to be tested at 5 kA.

It is the rectifier part, comprised of 4 superconducting switches, the one that is provided by the design proposal of this work, where it's needed to operate two switches simultaneously in order to gradually increase the current in the load. As mentioned in Chapter 4, a double switch configuration can be developed by connecting in series the top and bottom *ReBCO* tape segments, in this case with the inductive load in series between them.

Considering then the double switch configuration, the 5 kA current passes first through upper *ReBCO* tapes segment, then through the inductive load, and finally through the bottom *ReBCO* tapes segment. This means that it is needed a tapestack that overall can conduct 10 kA in order to handle the current in both ways. A safety factor also will be considered to ensure a reliable operation of the *ReBCO* switch.

6.2 10 kA rated ReBCO-based superconducting switch

Based on the computation of the 2D magnetic field for a high current tape stack, considering the 10 kA requirement, determines the number of *ReBCO* tapes required to conduct the aforementioned electric current. As it is needed to operate in a stable manner at this high current, a safety factor is considered, for which the design considers 12 kA as the critical current of the device. Then the *ReBCO* tapes, conducting 10 kA in total, will produce a magnetic field, and nevertheless be able to remain in the superconducting state.

Having a considerable margin in the operating temperature helps to reduce the total number of *ReBCO* tapes than if working closer from the critical temperature, as is the case with the first tests done with liquid nitrogen at 77 K. Then, the chosen temperature was settled up at 50 K, which allow to increase the critical current density in each tape, and then reduce the total number of *ReBCO* tapes necessary for handling the aimed 10 kA current. Reducing the operating temperature even further would allow to use less *ReBCO* tapes, however, this will also increase the temperature difference between the "closed" and "open" states, making the *ReBCO* switch slower.

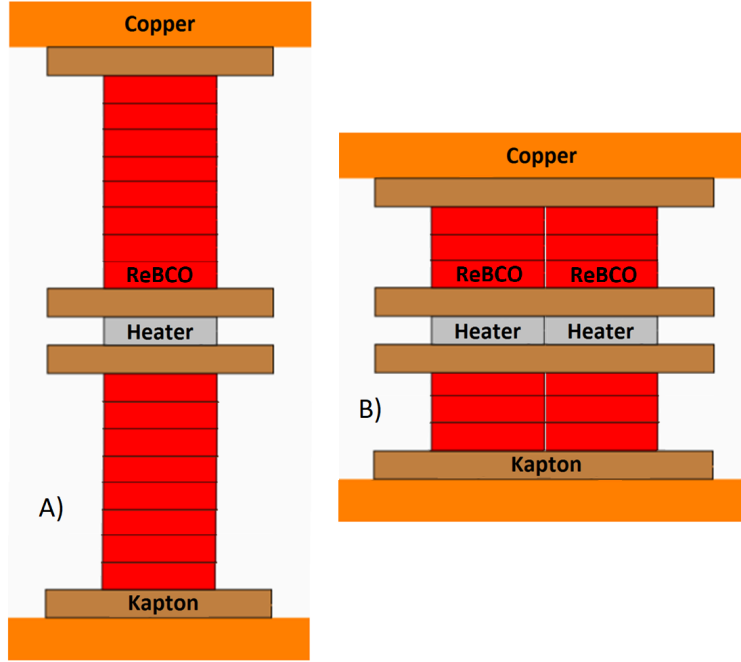


Figure 40: Options for a 10 kA ReBCO switch, considering an operating temperature of 50 K and 12 mm etched ReBCO tapes. A) Single vertical tapestack. B) Double tapestack.

The tests with the physical setup were done with tapes that have 4 mm in width, and where a single *ReBCO* tape is able to conduct about 150 A at 77 K. Reducing the operating temperature and making use of wider *ReBCO* tapes allow to determine a design that can handle the required electric current, for this case 12 mm tapes were chosen, which is the wider *ReBCO* tape option that can be purchased currently from the available provider [31].

The time response and technical specs are summarized in Table 3 and Table 4:

	A	B
τ_{delayR} [ms]	500	250
τ_{delayF} [ms]	100	60
τ_{rise} [ms]	50	20
τ_{fall} [ms]	10	10

Table 3: Time response for 10 kA ReBCO switch for both designs. The values presented are rounded.

	A	B
<i>Total HTS tapes</i>	16	12
<i>HTS tape width [mm]</i>	12	12
<i>Operating Temperature [K]</i>	50	50
<i>Temperature margin [K]</i>	2	2
<i>Open switch resistance [mΩ/m]</i>	37	50
<i>Total critical current [kA]</i>	13.61	13.65
<i>Heater power [W/m]</i>	3000	6000
<i>Switching frequency [Hz]</i>	1.4	3.3

Table 4: Technical specs for 10 kA ReBCO switch for both designs. The values presented are rounded.

As an explanation of stated values in Table 4:

- The temperature margin refers to a tolerance of two degrees above the operating temperature, for which the total critical current is still above the set value of 12 kA.
- The resistance and heater power values are given in values divided per unit length. This length is in the longitudinal direction of the tape, so perpendicular to the cross section of the tape stack. These values are normalized to this length, since an uniform process is assumed in this longitudinal direction.
- The switching frequency considers only the time response parameters for heating and cooling down of the tape stack. Additional time is needed during the operation of the *ReBCO* switch, e.g. transfer of the induced current from the secondary of the transformer to the inductive load, in a superconducting rectifier. Then, the switching frequency in a specific application will be slower than the indicated values in here.

Further comments about both designs are addressed in the following section.

7 Summary and Discussion

An overview of the outcomes of the project is presented, mentioning insights along the process and future work.

7.1 Summary

To predict the behavior of a thermally activated high current *ReBCO* switch, a simulation model in MATLAB was developed to test different configurations of *ReBCO* tape stacks, while changing the operating temperature of the device. The model considers the thermal response when a heat pulse is applied, where temperature and self generated magnetic field define the overall resistance of the *ReBCO* switch.

By using heat pulses as input in function of time is possible to change the superconducting state of the tapes, so parameters such as the cooling down time and time to change the superconducting state can be determined. Hence, the technical specifications for a particular configuration can be extracted. So in the simulation model different configurations can be tested, considering layers to be extended both in vertical and horizontal directions, in order to determine the one that has the best performance.

A *ReBCO* switch test stand was built by members of the superconductivity work group, and some tests and experimental data were already available when the development of the model started. This allowed then to compare the simulation results with the experimental data, which served as a validation during the modeling process. Then, in parallel to the simulation model development, the setup was gradually updated and additional measurements were obtained to further tune it.

The simulation model, at the last phase of the work, being able to compute the magnetic field for a high current flowing through a stack of *ReBCO* tapes, along with the thermal response in function of the control heat pulses, allowed to determine two proposals that are able to conduct the electric current goal of 10 kA at 50 K. One of them is wider, using 12 *ReBCO* tapes, and has a higher switching frequency. The other one is thinner, using 16 *ReBCO* tapes and consumes less power to operate than the first one, although the switching frequency is lower. Factors such as application, budget, as switching frequency and geometry requirements determine which option is chosen.

The experimental part of the project for a high current device, was not able to be developed on the time frame of this work. For one because of the problem to etch the *ReBCO* tapes in a consistent manner, which slowed the testing of tapestacks since the resistivity of the *ReBCO* tapes was varying from different tests. Also the learning process along lead to modifications in the experimental setup.

At the time this work was finished, the etching process was deemed reliable enough to have consistent etched samples, so a final 10 kA rated physical device seems to be on track to be developed on the short term, helped with the insights from the simulation model.

7.2 Discussion

Certain aspects respect the simulation model can be modified to have a more accurate description of the *ReBCO* switch operation. Similarly, a few aspects in the physical setup can be improved.

- *Update thermal model for 2D*

The physical setup was designed originally with the liquid nitrogen in contact only with the copper block, partially submerged, i.e. conduction cooling. In subsequent iterations of the test stand this design was modified, with a more compact copper casing, now totally submerged in liquid nitrogen, although the liquid nitrogen is not in direct contact due to an epoxy coating of the tape stack, there is an additional path for heat to propagate, both through the copper case and the epoxy coating. This then means that the cooling down of the setup would be faster, and a 2D thermal model would better describe the new setup than the actual one. This is, however, a positive outcome, since the switch seems will operate faster than what the 1D model can predict so far. Although the heat conductivity in some epoxy materials is relatively low compared to copper, it can be further investigated to take into account in the model.

- *Magnetic field anisotropy in model*

The computation of the current density in a superconductor is a function of both the temperature and magnetic field. In the case of the model, this is done by making a mesh along the width of the tape and computing the critical current at each point, taking into account its temperature and the total magnitude of the magnetic field in that point. However, this is an approximation, since there is the so called anisotropy of the magnetic field [59], i.e. the direction of the magnetic field respect with the plane of the *ReBCO* tape influences how much the critical current is reduced, being perpendicular to the surface when the effect is biggest. This means that the model can still be improved by adding this factor.

- *Etching of ReBCO tapes*

The best working scenario for a *ReBCO* switch is when the resistance at the "open" state is as high as possible. *ReBCO* tapes by fabric come with a copper coating to protect the superconducting material in case there is a loss of superconductivity, allowing the current to flow through it, considering that above the critical temperature the resistivity of the *ReBCO* material is considerably higher than copper. Then, for the *ReBCO* switch application, the copper coating is not desirable since it reduces the overall resistance of the *ReBCO* switch.

Etched *ReBCO* tapes can also be bought, but since custom *ReBCO* tape samples are required for the setup, the etching is done on site. The importance in removing the copper coating of the *ReBCO* tapes to increase the overall resistance of the *ReBCO* switch was realized early on in the project. However, this implies removing layers with a thickness of some tens of micrometers, and at the end of this work the method to remove them efficiently while conserving the superconducting properties of the tape was still on development. The latest tests indicate that the stabilizer layers can be removed in a seemingly consistent manner, so the etching method seem to be on good track in order to ultimately increase the overall resistance of the *ReBCO* switch.

- *Quench protection in physical setup*

While starting to increase the number of *ReBCO* tapes in the physical setup, some problems were encountered. The power source to inject the current in the setup was configured to be turned off when a certain threshold voltage was obtained (voltage produced when the *ReBCO* tapes become resistive and the electric current is running through them). However, without an external way to dissipate the energy, the power losses produced by the electric current in the heated *ReBCO* tapes surpassed the heat rate removal of the setup, so the tape stack was damaged. An external resistor or diode to protect the tape stack seems then necessary to dissipate the current and not to destroy the *ReBCO* tapes, which will need to be added in a subsequent phase of the project.

- *10 kA ReBCO switch design options*

There are some compromises to consider in order to choose for any of the options proposed, as well as insights regarding the technical specifications of the device.

- *Total price of the ReBCO switch*

The final price of the device will depend on the number of *ReBCO* tapes used, considering that currently it is expensive to produce compared with regular conducting or *LTS* cables. Under this consideration, the lower the number of *ReBCO* tapes used, the better, attainable when lowering the operating temperature.

- *Operating temperature considerations*

As known, the more distance between the operating point and the critical surface for the superconductor will mean having a wider range of values to work with. The self-magnetic field depends on the current that flows through the cable, this last parameter is the one that is wanted to be increased, which is done by decreasing the operating temperature. 77 K would be a convenient temperature to operate because of the low price of liquid nitrogen, but the window margin at those conditions requires a high number of tapes, increasing the cost and slowing the time response due to an increased thermal resistance.

A very low temperature (4 K with liquid helium), while it reduces the number of *ReBCO* tapes needed, it also increase the operating power and time delays due to the wide temperature range that needs to be traversed to quench the tape, along with the higher cost of the coolant.

For these compromising factors, 50 K was selected as the temperature for the device to operate in both proposed configurations, using a reasonable number of HTS tapes while not affecting too much the time delays when heating and cooling down the device, when switching between "closed" and "open" states. This also eliminates the need of using liquid helium as a coolant.

- *Geometric characteristics*

Testing of superconducting technology is usually done in some enclosed vessel or facility designed to maintain a low temperature, which depending on the required temperature, can be operated from coolants ranging from liquid nitrogen to liquid helium. Hence, there is a limitation in the size that a testing unit as a total can have so it fits inside the facility. Then, this restriction gets defined as a whole depending on the application and available testing facilities.

The chosen width of the tapes is 12 mm, to have a wider cross section area and increase the overall current density, which allow to choose between one and two horizontal stacks in designs "A" and "B", while being able to handle the 10 kA current specification.

The length is a parameter that has a linear dependence in power consumption and overall resistivity of the *ReBCO* switch, as well as on the cost considering a proportional increase in price per meter. A length of 15 cm was chosen for making the first tests in the experimental setup, although this became slightly shorter or larger in subsequent tests. This factor can be further investigated to find a good compromise between the values mentioned, which again, depend on the characteristics and requirements of the application in mind.

– *Power consumption and switch speed*

Usually it is desired for any electric device to consume the least amount of power possible. In the case of the proposals provided, design "A" consumes less power to operate than design "B", however, "A" is also a slower switch due to the decreased heat propagation rate, result of having more *ReBCO* tapes between the heat source and heat sink, making "B" a better design in the matter of the switching speed. But, on the other hand, heat is also a factor to be minimized in cryogenic systems, and although "B" is a faster switch, the power needed to operate the device might disrupt the cryogenic system if its cooling rate is not enough to compensate for it, plus the increase in cryogenic fluid consumption (relatively cheap if liquid nitrogen is used, but expensive if working with liquid helium).

– *Switching frequency*

The maximum switching frequency for the device was stated for the 10 kA design, which is the fastest that the switch can be operated in one cycle with a heat pulse, while returning to the nominal cold temperature after being heated up. In the experimental test, however, it was observed that even if the switch was cold again, it was required an extra time to recover the zero resistivity state (a few hundreds of milliseconds). This factor needs to be further investigated, meaning that the switching frequency will be lower due to this extra time parameter.

A superconducting switch operates on the principle than when it is "opened", the electric current is redirected towards another superconducting line connected in parallel or a less resistive path, such as an external dump resistor. Assuming the second case, the lower the ratio of superconducting switch resistance to dump resistance, the more power will be dissipated in the superconducting switch due to the Joule effect.

In the experimental setup there is a switching off of the current source when a threshold voltage is detected across the *ReBCO* switch. However, an external dump resistor was not installed as an additional safety measure. This means that the main superconducting current will be dissipated in the *ReBCO* switch when it is "opened" as long as the voltage detected is not high enough. This is the likely reason that the experimental setup took slightly longer to cool down, since there was a partially resistive part of the *ReBCO* material that was still generating heat when the device was being cooled down.

Scaling to higher currents seems to mean that it is necessary to install an external

dump resistor or diode because, even if the high current is interrupted relatively quickly, for a short amount of time there will be a high power generated in the *ReBCO* tapes that can damage the setup if they are only being dissipated in a high resistance element.

Based on the previous points, then we return to address the research question and subquestions and give on-the-point answers to them, in the framework of this project.

- *Can a 10 kA thermally activated superconducting switch be developed with HTS tapes technology, with a switching frequency of 1 Hz?*

Scaling the experimental setup developed with more *ReBCO* tapes it is deemed feasible in the short term to reach the 10 kA goal, given further testing and gradual increase of the number of *ReBCO* tapes. Refining the etching process will also allow to increase in a consistent manner the resistance of the *ReBCO* switch.

The speed of the device is dependent on the heat propagation rate of the device, both when getting heated up and cooled down. These time values increase when operating at lower temperatures and increasing the number of *ReBCO* tapes. Based on the results of the model, attaining a switching frequency of the order of 1 Hz is possible for a high current device, but it needs to be validated in a physical setup.

It depends on the application of the *ReBCO* switch if this is fast enough for its purpose. For a quench protection system the switch speed is crucial, to quickly divert the stored energy of the superconducting coil in an external resistor. In a superconducting rectifier this is a less constraining requirement, meaning a longer time to charge or discharge a superconducting coil, but otherwise not critical regarding the safety or operation of the device.

- *What is an adequate temperature for the ReBCO switch to operate?*

For the proposed configurations, 50 K was chosen to be the best temperature to operate, to keep low the number of *ReBCO* tapes and avoid using liquid helium as coolant, as well as reducing the impact on the speed of the *ReBCO* switch by having a too big temperature gap between closed and open states.

- *Is the influence of magnetic field produced by the high current manageable in a multiple ReBCO tapes scenario?*

Considering the self magnetic field is fundamental since it reduces the operational window of superconductivity. As shown, this can be coped within a *ReBCO* tape stack and achieve the electric current goal.

- *Are parallel connected ReBCO tapes sufficient or is it necessary to opt for an alternate high current HTS cable?*

At the status date of the project, for this prototype and in order to reach the 10 kA goal, it doesn't seem necessary to opt for a high current *ReBCO* cable instead of the stacked *ReBCO* tapes. However, for making a final design that is connected in a superconducting circuit, where joints are needed to connect the segments, this idea would need revising in a final application, for assembly compatibility and manufacture purposes.

8 Conclusion

The aim of this project is to provide renewed support in the applications of the superconducting switch idea formerly developed for LTS. Nowadays, the commercial availability of *HTS* materials allow to revise it (ReBCO for the case of this project), having now a wider temperature and magnetic field margins to operate, enhancing the stability of the device.

The development of this technology is relevant for handling the current that flows through a superconducting coil, considering the possibility to redirect the current in the case of an accidental loss of the superconducting state (quench protection systems for superconducting coils with a high stored energy) as well as to charge and discharge gradually the coil with a low current power source (superconducting rectifier).

A simulation model was developed in the MATLAB environment to test different operating temperature scenarios and geometric arrangements, validated with experimental data in a low current device. The model can describe the thermal evolution to a time dependent heat pulse, for which the resistance of the switch can be varied to change from "closed" (zero resistance) to "open " (high resistance) states when surpassing the critical temperature. The detrimental effect of the magnetic field in critical current density is included, which needs to be taken into account in a high current device.

The code allow to design then a *ReBCO* switch in multiple configurations, and test them in a variety of operating conditions, as well as extracting the technical specifications. The *ReBCO* switch designs presented in this work, based on the agreement achieved comparing with the experimental data for a low current setup, are expected to behave similarly for the high current scenario. However, the designs given are a guideline, which need to be validated by a corresponding high current physical device.

Further experimental tests are necessary to keep increasing the current handling capabilities of the tape stack presented in this work, as well as a consistent way to etch the *ReBCO* tapes. Once having a fully working *ReBCO* switch for high current, an alternate option will be available to control the current direction that runs through a superconducting coil.

Acknowledgements

To my family for all their support.

To all the friends and colleagues that I met during these last two years, thank you for the good times, it is being a pleasure to get to know a bit from people from all around the globe.

To my supervisors Niek Lopes and Herman ten Kate, who gave me the opportunity to collaborate in this project at CERN, and get a glimpse on superconductivity R&D. To Nikolay Bykovskiy and Alexey Dudarev, with whom I collaborated for the realization of this project, as well as all the members of the EP-ADO work group for their help and fruitful discussions.

To the CONACYT (Consejo Nacional de Ciencia y Tecnología) Abroad Scholarship Program from Mexico and the Amandus H. Lundqvist Scholarship Program from Netherlands, which provided the funding that allowed me to support my studies.

To FuseNet (European Fusion Education Network) for the travel funding support during my stay in CERN for the realization of this project.

References

- [1] Giuliano Buceti. “Sustainable power density in electricity generation”. In: *Management of Environmental Quality: An International Journal* 25.1 (2014), pp. 5–18. DOI: 10.1108/MEQ-05-2013-0047. eprint: <https://doi.org/10.1108/MEQ-05-2013-0047>. URL: <https://doi.org/10.1108/MEQ-05-2013-0047>.
- [2] Ioannis N. Kessides. “Nuclear Power and Sustainable Energy Policy: Promises and Perils”. In: *The World Bank Research Observer* 25.2 (2010), pp. 323–362. DOI: 10.1093/wbro/lkp010. eprint: [/oup/backfile/content_public/journal/wbro/25/2/10.1093/wbro/lkp010/2/lkp010.pdf](http://oup/backfile/content_public/journal/wbro/25/2/10.1093/wbro/lkp010/2/lkp010.pdf). URL: <http://dx.doi.org/10.1093/wbro/lkp010>.
- [3] Akos Horvath and Elisabeth Rachlew. “Nuclear power in the 21st century: Challenges and possibilities”. In: *Ambio* 45.1 (Jan. 2016), pp. 38–49. ISSN: 1654-7209. DOI: 10.1007/s13280-015-0732-y. URL: <https://doi.org/10.1007/s13280-015-0732-y>.
- [4] Christian Barth. “High Temperature Superconductor Cable Concepts for Fusion Magnets”. 31.03.04; LK 01. PhD thesis. 2013. 232 pp. ISBN: 978-3-7315-0065-0. DOI: 10.5445/KSP/1000035747.
- [5] D.G. Schlom and J. Mannhart. “High-temperature Superconductors: Thin Films and Multilayers”. In: *Encyclopedia of Materials: Science and Technology*. Ed. by K.H. Jürgen Buschow et al. Oxford: Elsevier, 2001, pp. 3806–3819. ISBN: 978-0-08-043152-9. DOI: <https://doi.org/10.1016/B0-08-043152-6/00678-1>. URL: <http://www.sciencedirect.com/science/article/pii/B0080431526006781>.
- [6] J. C. Hernandez-Llambes and D. Hazelton. “Advantages of second-generation high temperature superconductors for pulsed power applications”. In: *2009 IEEE Pulsed Power Conference*. June 2009, pp. 221–226. DOI: 10.1109/PPC.2009.5386312.
- [7] Stephen A. Gourlay et al. “Superconducting Magnets and Their Applications”. In: *ChemInform* 36.25 (). DOI: 10.1002/chin.200525291. eprint: <https://onlinelibrary.wiley.com/doi/pdf/10.1002/chin.200525291>. URL: <https://onlinelibrary.wiley.com/doi/abs/10.1002/chin.200525291>.
- [8] K Vinod, R G Abhilash Kumar and U Syamaprasad. “Prospects for MgB₂ superconductors for magnet application”. In: *Superconductor Science and Technology* 20.1 (2007), R1. URL: <http://stacks.iop.org/0953-2048/20/i=1/a=R01>.
- [9] A.I. Golovashkin et al. “Low temperature direct measurements of Hc₂ in HTSC using megagauss magnetic fields”. In: *Physica C: Superconductivity* 185-189 (1991), pp. 1859–1860. ISSN: 0921-4534. DOI: [https://doi.org/10.1016/0921-4534\(91\)91055-9](https://doi.org/10.1016/0921-4534(91)91055-9). URL: <http://www.sciencedirect.com/science/article/pii/0921453491910559>.
- [10] Laan van der D. C et al. “Temperature and magnetic field dependence of the critical current of BiSrCaCuO tape conductors”. In: (Jan. 2001), pp. 3345–3348.
- [11] M. K. Wu et al. “Superconductivity at 93 K in a new mixed-phase Y-Ba-Cu-O compound system at ambient pressure”. In: *Phys. Rev. Lett.* 58 (9 Mar. 1987), pp. 908–910. DOI: 10.1103/PhysRevLett.58.908. URL: <https://link.aps.org/doi/10.1103/PhysRevLett.58.908>.

- [12] Jun Nagamatsu et al. “Superconductivity at 39 K in magnesium diboride”. In: *Nature* 410 (Mar. 2001), URL: <http://dx.doi.org/10.1038/35065039>.
- [13] Tsuyoshi Sekitani, Yasuhiro H Matsuda and Noboru Miura. “Measurement of the upper critical field of optimally-doped YBa₂Cu₃O_{7-d} in megagauss magnetic fields”. In: *New Journal of Physics* 9.3 (2007), p. 47. URL: <http://stacks.iop.org/1367-2630/9/i=3/a=047>.
- [14] H. W. Weijers et al. “High Field Magnets With HTS Conductors”. In: *IEEE Transactions on Applied Superconductivity* 20.3 (June 2010), pp. 576–582. ISSN: 1051-8223. DOI: 10.1109/TASC.2010.2043080.
- [15] Franco Julio Mangiarotti. *Design of Demountable Toroidal Field Coils with REBCO Superconductors for a Fusion Reactor*. Massachusetts Institute of Technology, 2016.
- [16] Jeffrey P Freidberg. *Plasma Physics and Fusion Energy*. Cambridge University Press, 2008.
- [17] G.B.J. Mulder et al. “Development of a thermally switched superconducting rectifier for 100 kA”. In: *IEEE transactions on magnetics* 27.2 (1991), pp. 2333–2336. ISSN: 0018-9464. DOI: 10.1109/20.133685.
- [18] Vyacheslav F. Solovyov and Qiang Li. “Fast high-temperature superconductor switch for high current applications”. In: *Applied Physics Letters* 103.3 (2013), p. 032603. DOI: 10.1063/1.4813883. eprint: <https://doi.org/10.1063/1.4813883>. URL: <https://doi.org/10.1063/1.4813883>.
- [19] Jeremy D. Weiss et al. “Introduction of CORC[®] wires: highly flexible, round high-temperature superconducting wires for magnet and power transmission applications”. In: *Superconductor Science and Technology* 30.1 (Nov. 2016). DOI: 10.1088/0953-2048/30/1/014002.
- [20] Danko van der Laan et al. *High-field magnets wound from CORC[®] cables and wires*. CHATS on Applied Superconductivity 2017. Sendai, Japan. Dec. 2017.
- [21] Tim Mulder et al. *REBCO CORC Wire and Cable-In-Conduit Conductor Development at CERN*. Barcelona, Spain. Feb. 2017.
- [22] T Mulder et al. “Design and Preparation of Two ReBCO-CORC[®] Cable-In-Conduit Conductors for Fusion and Detector Magnets”. In: *IOP Conference Series: Materials Science and Engineering* 279.1 (2017), p. 012033. URL: <http://stacks.iop.org/1757-899X/279/i=1/a=012033>.
- [23] Simon Alastair Keys. *Temperature and strain scaling laws for the critical current density in Nb₃Sn and Nb₃Al conductors in high magnetic fields*. Durham University, 2001. URL: <http://etheses.dur.ac.uk/3951/>.
- [24] P.H. Kes. “Electrodynamics of Superconductors: Flux Properties”. In: *Encyclopedia of Materials: Science and Technology*. Ed. by K.H. Jürgen Buschow et al. Oxford: Elsevier, 2001, pp. 2535–2537. ISBN: 978-0-08-043152-9. DOI: <https://doi.org/10.1016/B0-08-043152-6/00459-9>. URL: <http://www.sciencedirect.com/science/article/pii/B0080431526004599>.
- [25] M.N. Wilson. *Superconducting Magnets*. Monographs on cryogenics. Clarendon Press, 1983. ISBN: 9780198548102. URL: <https://books.google.nl/books?id=A0bvAAAAAAJ>.

- [26] Bryan Luther. *Superconductivity: Basic Properties*. <http://faculty.cord.edu/luther/physics225/lectures/superconductors.pdf>. (Accessed on 10/08/2018).
- [27] J. Pereiro et al. “Insights from the study of high-temperature interface superconductivity”. In: *Philosophical Transactions of the Royal Society of London A: Mathematical, Physical and Engineering Sciences* 370.1977 (2012), pp. 4890–4903. ISSN: 1364-503X. DOI: 10.1098/rsta.2012.0219. eprint: <http://rsta.royalsocietypublishing.org/content/370/1977/4890.full.pdf>. URL: <http://rsta.royalsocietypublishing.org/content/370/1977/4890>.
- [28] J. W. Ekin. “Offset criterion for determining superconductor critical current”. In: *Applied Physics Letters* 55.9 (1989), pp. 905–907. DOI: 10.1063/1.102259. eprint: <https://doi.org/10.1063/1.102259>. URL: <https://doi.org/10.1063/1.102259>.
- [29] *IEC 61788-1:2006 | IEC Webstore*. <https://webstore.iec.ch/publication/5909>. (Accessed on 10/08/2018).
- [30] Saul Rindt. *Development of the First ReBCO-CORC Based Racetrack Model Coil*. Eindhoven University of Technology, 2018.
- [31] *Wire Specification | SuperPower*. <http://www.superpower-inc.com/content/wire-specification>. (Accessed on 10/03/2018).
- [32] Makoto Takayasu et al. “HTS twisted stacked-tape cable conductor”. In: *Superconductor Science and Technology* 25.1 (2012), p. 014011. URL: <http://stacks.iop.org/0953-2048/25/i=1/a=014011>.
- [33] Wilfried Goldacker et al. “Roebel cables from REBCO coated conductors: a one-century-old concept for the superconductivity of the future”. In: *Superconductor Science and Technology* 27.9 (2014), p. 093001. URL: <http://stacks.iop.org/0953-2048/27/i=9/a=093001>.
- [34] D Uglietti, Rainer Wesche and Pierluigi Bruzzone. “Design and Strand Tests of a Fusion Cable Composed of Coated Conductor Tapes”. In: 24 (June 2014), pp. 1–4.
- [35] G. Celentano et al. “Design of an Industrially Feasible Twisted-Stack HTS Cable-in-Conduit Conductor for Fusion Application”. In: *IEEE Transactions on Applied Superconductivity* 24.3 (June 2014), pp. 1–5. ISSN: 1051-8223. DOI: 10.1109/TASC.2013.2287910.
- [36] Y. Terazaki et al. “Measurement and Analysis of Critical Current of 100-kA Class Simply-Stacked HTS Conductors”. In: *IEEE Transactions on Applied Superconductivity* 25.3 (June 2015), pp. 1–5. ISSN: 1051-8223. DOI: 10.1109/TASC.2014.2377793.
- [37] M. J. Wolf et al. “HTS CroCo: A Stacked HTS Conductor Optimized for High Currents and Long-Length Production”. In: *IEEE Transactions on Applied Superconductivity* 26.2 (Mar. 2016), pp. 19–24. ISSN: 1051-8223. DOI: 10.1109/TASC.2016.2521323.
- [38] W. H. Fietz et al. “High-Current HTS Cables: Status and Actual Development”. In: *IEEE Transactions on Applied Superconductivity* 26.4 (June 2016), pp. 1–5. ISSN: 1051-8223. DOI: 10.1109/TASC.2016.2517319.
- [39] Yeekin Tsui, Elizabeth Surrey and Damian Hampshire. “Soldered joints—an essential component of demountable high temperature superconducting fusion magnets”. In: *Superconductor Science and Technology* 29.7 (2016), p. 075005. URL: <http://stacks.iop.org/0953-2048/29/i=7/a=075005>.

- [40] Gourab BANSAL et al. “High-Temperature Superconducting Coil Option for the LHD-Type Fusion Energy Reactor FFHR”. In: *Plasma and Fusion Research* 3 (2008), S1049–S1049. DOI: 10.1585/pfr.3.S1049.
- [41] F. J. Mangiarotti and J. V. Minervini. “Advances on the Design of Demountable Toroidal Field Coils With REBCO Superconductors for an ARIES-I Class Fusion Reactor”. In: *IEEE Transactions on Applied Superconductivity* 25.3 (June 2015), pp. 1–5. ISSN: 1051-8223. DOI: 10.1109/TASC.2014.2379641.
- [42] B.N. Sorbom et al. “ARC: A compact, high-field, fusion nuclear science facility and demonstration power plant with demountable magnets”. In: *Fusion Engineering and Design* 100 (2015), pp. 378–405. ISSN: 0920-3796. DOI: <https://doi.org/10.1016/j.fusengdes.2015.07.008>. URL: <http://www.sciencedirect.com/science/article/pii/S0920379615302337>.
- [43] T.S. Lee et al. “Optimal design of a toroidal field magnet system and cost of electricity implications for a tokamak using high temperature superconductors”. In: *Fusion Engineering and Design* 98-99 (2015). Proceedings of the 28th Symposium On Fusion Technology (SOFT-28), pp. 1072–1075. ISSN: 0920-3796. DOI: <https://doi.org/10.1016/j.fusengdes.2015.06.125>. URL: <http://www.sciencedirect.com/science/article/pii/S0920379615301526>.
- [44] V S Vysotsky et al. “The possibility of using high-T_c superconducting films as elements of a rectifier”. In: *Superconductor Science and Technology* 3.5 (1990), p. 259. URL: <http://stacks.iop.org/0953-2048/3/i=5/a=009>.
- [45] E. Lu C. Neumeyer G. Bronner and S. Rarnakrishnan. “Quench Protection Circuits for Superconducting Magnets”. In: (1995). URL: <http://ieeexplore.ieee.org/abstract/document/534459/>.
- [46] Chris Llewellyn Smith and Steve Cowley. “The path to fusion power”. In: *Philos Trans A Math Phys Eng Sci* 368.1914 (Mar. 2010). 20123748[pmid], pp. 1091–1108. ISSN: 1364-503X. DOI: 10.1098/rsta.2009.0216. URL: <http://www.ncbi.nlm.nih.gov/pmc/articles/PMC3263804/>.
- [47] R.G. Sharma. *Superconductivity: Basics and Applications to Magnets*. Springer Series in Materials Science. Springer International Publishing, 2015. ISBN: 9783319137131. URL: <https://books.google.nl/books?id=jbvdbgAAQBAJ>.
- [48] Cryomagnetics Inc. *Basics of Superconducting Magnets*. https://www.cryomagnetics.com/wp-content/uploads/reference/Basics_of_Superconducting_Magnets.pdf. Online; accessed 12 April 2018.
- [49] Herman H.J. ten Kate et al. “High current and high power superconducting rectifiers”. In: *Cryogenics* 21.5 (1981), pp. 291–269. ISSN: 0011-2275. DOI: 10.1016/0011-2275(81)90006-0.
- [50] L.J.M. van de Klundert and H.H.J. ten Kate. “On fully superconducting rectifiers and fluxpumps. A review. Part 2: Commutation modes, characteristics and switches”. In: *Cryogenics* 21.5 (1981), pp. 267–277. ISSN: 0011-2275. DOI: [https://doi.org/10.1016/0011-2275\(81\)90002-3](https://doi.org/10.1016/0011-2275(81)90002-3). URL: <http://www.sciencedirect.com/science/article/pii/0011227581900023>.
- [51] Nikolay Bykovskiy. *BabyIAXO Design Update Presentation*. Mar. 2018.

- [52] Jianzhao Geng. “Flux Pumping for High-Tc Superconducting (HTS) Magnets”. PhD thesis. Nov. 2017.
- [53] L. M. Barkov et al. “Superconducting rectifier fluxpump for magnet system of the CMD-2 detector”. In: *IEEE Transactions on Applied Superconductivity* 9.3 (Sept. 1999), pp. 4585–4590. ISSN: 1051-8223. DOI: 10.1109/77.791914.
- [54] J. Sikkenga and H. H. J. ten Kate. “A full scale superconducting rectifier for powering an MRI-magnet”. In: *IEEE Transactions on Magnetism* 25.2 (Mar. 1989), pp. 1771–1774. ISSN: 0018-9464. DOI: 10.1109/20.92644.
- [55] A. V. Dudarev et al. “Quench protection of very large superconducting magnets”. In: *IEEE Transactions on Applied Superconductivity* 5.2 (June 1995), pp. 226–229. ISSN: 1051-8223. DOI: 10.1109/77.402530.
- [56] L.J.M. van de Klundert and Herman H.J. ten Kate. “Fully superconducting rectifiers and fluxpumps Part 1: Realized methods for pumping flux”. In: *Cryogenics* 21.4 (1981), pp. 195–206. ISSN: 0011-2275. DOI: 10.1016/0011-2275(81)90195-8.
- [57] Y.A. Çengel. *Heat and Mass Transfer: A Practical Approach*. Heat and Mass Transfer: A Practical Approach. McGraw-Hill, 2007. URL: <https://books.google.nl/books?id=WgZaAAAAYAAJ>.
- [58] N Bykovsky et al. “Magnetization loss for stacks of ReBCO tapes”. In: *Superconductor Science and Technology* 30.2 (2017), p. 024010. URL: <http://stacks.iop.org/0953-2048/30/i=2/a=024010>.
- [59] E. Pardo et al. “Low-magnetic-field dependence and anisotropy of the critical current density in coated conductors”. In: 24.6 (2011), p. 10. ISSN: 0953-2048. URL: <http://dx.doi.org/10.1088/0953-2048/24/6/065007>.